Modeling metal ion-humic substances complexation in highly saline conditions

Rémi M Marsac, Nidhu L Banik, Johannes L Lützenkirchen, Charlotte Catrouillet, Christian M Marquardt, Karen H Johannesson

Accepted Manuscript

Modeling metal ion-humic substances complexation in highly saline conditions

Rémi Marsac, Nidhu L. Banik, Johannes Lützenkirchen, Charlotte Catrouillet, Christian M. Marquardt, Karen H. Johannesson

PII: S0883-2927(16)30231-1

DOI: 10.1016/j.apgeochem.2017.02.004

Reference: AG 3821

To appear in: *Applied Geochemistry*

Received Date: 19 August 2016

Revised Date: 23 January 2017

Accepted Date: 1 February 2017

Please cite this article as: Marsac, R., Banik, N.L., Lützenkirchen, J., Catrouillet, C., Marquardt, C.M., Johannesson, K.H., Modeling metal ion-humic substances complexation in highly saline conditions, *Applied Geochemistry* (2017), doi: 10.1016/j.apgeochem.2017.02.004.

Modeling metal ion-humic substances complexation in highly saline conditions

Rémi Marsac[1,2,*], Nidhu L. Banik[2,3], Johannes Lützenkirchen[2], Charlotte Catrouillet[1], Christian M. Marquardt[2], Karen H. Johannesson[4]

*Corresponding author: e-mail address: remi.marsac@univ-rennes1.fr
Tel: +332 23 23 53 56. Fax: +332 23 23 60 90
[1]Géosciences Rennes UMR 6118, Université Rennes 1, CNRS, 35042 Rennes cedex, France.
[2]Institute for Nuclear Waste Disposal, Karlsruhe Institute of Technology, P.O. Box 3640, D-76021 Karlsruhe, Germany.
[3]JRC-KARLSRUHE, G.II.6 - Nuclear Safeguards and Forensics, European Commission, P.O.Box 2340, D-76125 Karlsruhe
[4]Department of Earth and Environmental Sciences, Tulane University, 6823 St. Charles Avenue, New Orleans, LA 70118, USA.

Highlights:

- Model VII and NICA-Donnan are tested at high ionic strength (*I*) using the SIT.
- For *I* > 1 m, Model VII is applicable as a non-electrostatic model.
- No modification is needed for NICA-Donnan.
- Both models predict the effect of *I* on proton- and metal ion-humate (M-HA) binding.
- SIT parameters for simpler M-HA binding models vary with pH and metal loading.

Abstract. Because highly saline groundwaters are found at potential repository sites for nuclear waste, geochemical models should predict the speciation of relevant radionuclides in brines, including their complexation with substances such as humic acids (HA). In this study, available experimental radionuclide-HA complexation data in high 1:1 background electrolyte solutions ($0.01 < m_{\mathrm{NaCl}/NO_3/\mathrm{ClO_4}} < 4$ molal, *m)* are reviewed. Discrepancies in the amplitude of ionic strength effects on radionuclide-HA complexation are observed, which might depend on the nature of the interacting radionuclide or on the origin of HA. However, significant differences in the experimental conditions and calculations applied to determine conditional metal ion-HA complexation constants hamper direct comparison between these datasets. To clarify whether metal ion-HA binding in saline solutions can be described, two sophisticated humic-ion binding models (Model VII and NICA-Donnan) are presently used. This is the first time that Model VII and NICA-Donnan are applied to predict metal ion-HA binding at high ionic strength (I > 1 m). The advantage of these models, compared to more simple ones (e.g., the polyelectrolyte or the charge neutralization models), is that both electrostatic and chemical contributions to the overall metal ion-HA binding are explicitly taken into account. Model VII and NICA-Donnan are shown to produce very similar results. Trends in conditional metal ion-HA binding constants and in the maximum metal ion uptake by HA (e.g., the loading capacity) with I agree with experiments. The present data evaluation suggests that most of the apparent discrepancies between various experimental datasets arise from differences in the experimental conditions. Both Model VII and NICA-Donnan predict that the specific ion interaction theory (SIT) parameters for metal ion-HA systems, which are required for high ionic strength with more simple models, vary with pH and metal loading. Overall, Model VII and NICA-Donnan are able to account for various mechanisms involved in metal ion-HA complexation, including the metal loading effects and cation

competition, and might be helpful predictive tools for performance safety assessment up to highly saline conditions.

Keywords: humic, radionuclide, complexation, brine, saline, Model VII, NICA-Donnan, specific ion interaction theory.

1. Introduction

Humic substances (HS) such as humic (HA) and fulvic (FA) acids are ubiquitous in natural waters and form complexes with dissolved metal ions. They play a crucial role for metal ion mobility and bioavailability in the environment. HS exhibit extreme complexity. The major HS cation-binding groups are the carboxylic and phenolic groups (Ritchie and Perdue, 2003), but less abundant softer Lewis bases (e.g., N- and S-containing groups) also contribute to cation-HS complexation (Tipping, 1998; Hesterberg et al., 2001). HS are macro-ions and electrostatic effects are relevant for their complexation properties. Moreover, several HS groups may bind a single cation, which either leads to a chelation effect (Martell and Hancock, 1996) or to the formation of a cation bridge between different organic molecules (e.g., Kunhi Mouvenchery et al., 2012). Hence, metal ions can form a large variety of complexes with HS, leading to apparent complexation constants that depend on pH, ionic strength and metal ion/HS concentration ratio (i.e., the metal loading) including the presence of competing cations like Ca and Mg. Substantial efforts have been made to determine thermodynamic metal ion-HS complexation constants and to develop predictive models for environmentally relevant conditions (e.g., Kim and Czerwinski, 1996; Benedetti et al., 1995; Tipping, 1998; Milne et al., 2001; 2003; Sasaki et al., 2008). Because of the complexity of HS, very different approaches have been proposed to describe the reaction between HS and metal ions.

The resulting metal ion-HS complexation models were developed for, and mainly applied to describe metal ion speciation under freshwater conditions, but were shown to be applicable for the more saline conditions that occur in estuaries and seawaters (e.g., Hiemstra and van Riemsdijk, 2006; Turner et al., 2008; Stockdale et al., 2011). Nonetheless, few studies have investigated metal ion-HS interactions under highly saline conditions, such as ionic strength (I) exceeding that of seawater (i.e., $I > 0.7$ m). The latter conditions are relevant with regard to the

safety of nuclear waste disposal in rock salt formationsor in specific clay formations. For example, deep waters in the Jurassic and lower Cretaceaous clay rock formations in Northern Germany may contain salt concentrations as high as about 4 M (Mühlenberg et al., 1997). Sedimentary rocks currently investigated in Canada are in contact with brine solutions up to 6.5 M (Fritz and Frape, 1982). Although high ionic strength commonly leads to the coagulation of HS, this process has been shown to be incomplete in many cases and non-negligible amounts of dissolved HS were reported to persist (Wall and Choppin, 2003), which can react with dissolved metal ions.

Most of the radionuclide-HS complexation studies in saline solutions focused on HA. Because few data for FA exist, only HA binding properties at high ionic strength are discussed herein. Generally, at constant pH, the apparent radionuclide-HA complexation constants in monovalent background electrolyte solutions (e.g., NaCl or $NaClO_4$) decrease with increasing ionic strength from very dilute aqueous solutions up to 1 molal (mol kg^{-1}, hereafter denoted *m*). However, different binding behaviors are observed for $I > 1$ *m*. Specifically, UO_2^{2+}- and Pu^{4+}-HA complexation constants increase with increasing ionic strength (Labonne-Wall et al., 1999; Szabò et al., 2010), whereas Co^{2+}-HA complexation does not vary substantially, and Ni^{2+}-HA complexation slightly decreases (Kurk and Choppin, 2000) with increasing ionic strength. Although data from Czerwinski et al. (1996) and Wall et al. (2002) consistently show increasing Am^{3+}/Cm^{3+}-HA binding with increasing *I*, Czerwinski et al. (1996) observed minor variation in complexation constant values with *I*. This led them to propose an average value (with standard variation of ± 0.14 log units) for the entire range of *I* investigated, which contrasts with Wall et al. (2002) where much larger variations were reported (about 3 log units). Furthermore, for $1 \leq I \leq 3.5$ *m*, the maximum amount of radionuclide that is experimentally found to bind to HA (e.g., the so called loading capacity in the charge neutralization model) was shown to decrease with

106 increasing *I* for trivalent actinides (Czerwinski et al., 1996), whereas it remained constant in the
107 case of Pu(IV) (Szabò et al., 2010). All these discrepancies might be indicative of conformational
108 changes in saline solutions, which would depend on the nature of the interacting radionuclide as
109 well as on the origin of HA. However, significant differences exist in the experimental conditions
110 and calculations applied to determine conditional metal ion-HA complexation constants between
111 these different studies, which complicates data comparison. Some studies were conducted in non-
112 complexing background electrolyte solutions ($NaClO_4$; Czerwinski et al., 1996; Szabò et al.,
113 2010). High [Cl^-] is environmentally relevant (as opposed to high [ClO_4^-]), but metal ions can
114 bind Cl^-, which may affect the determination of radionuclide-HA complexation constants.
115 Complexation data for UO_2^{2+}- and Am^{3+}-HA binding from Labonne-Wall et al. (1999) and Wall
116 et al. (2002) were obtained in acetate buffers under ambient (air) atmosphere. Like many ligands,
117 acetate and carbonate form aqueous complexes with UO_2^{2+} and Am^{3+} and can compete with HA.
118 Experiments were conducted at different radionuclide-to-HA concentration ratios, which might
119 also affect HA charge and conformation. Finally, pH measurement is non-trivial in saline
120 solutions. More specifically, "constant pH values" can refer to constant proton activity (pH = -
121 log a_{H^+}; Szabò et al., 2010), proton molality (pH_m = - log m_{H^+}; Czerwinski et al., 1996;
122 Labonne-Wall et al., 1999; Wall et al., 2002), or constant experimental values, as read on the pH-
123 meter (pH_{exp}; Kurk and Choppin, 2000; where the pH_{exp}-pH_m relationship is provided). Deviation
124 between pH, pH_m and pH_{exp} as affected by *I* may also hamper comparison between different
125 datasets.

126 Available radionuclide-HA complexation data have been analyzed using relatively simple
127 models such as the Polyelectrolyte Model (PM; Torres and Choppin, 1984) or the Charge
128 Neutralization Model (CNM; Kim and Czerwinski, 1996). These models can be conveniently
129 included in the speciation codes used for performance safety assessment. Within these models,

130 binding parameters may vary with pH and *I*. High salt levels require an appropriate treatment of
131 activity coefficients for aqueous species in geochemical models, such as application of specific
132 ion interaction theory (SIT; Ciavatta, 1980). Metal-HA complexation constants can also be
133 extrapolated to $I = 0$ using SIT, when considering HA as a solute. However, due to HA
134 complexity, SIT parameters are no more than adjustable parameters and their values have no
135 clear physical significance according to the original authors (Czerwinski et al., 1996; Szabò et al.,
136 2010). Given the differences in the experimental conditions between previous radionuclide-HA
137 complexation studies and the different calculations applied for the determination of metal-HA
138 complexation constants (e.g., with the CNM or the PM), it is difficult to evaluate how SIT
139 parameters would evolve with changing metal ion concentrations and physico-chemical
140 conditions.

141 More sophisticated models exist, such as the humic ion binding Model VII (Tipping et al.,
142 2011), or its previous versions (Models V/VI: Tipping and Hurley, 1992; Tipping, 1998), and the
143 NICA-Donnan model (Kinniburgh et al., 1996; Koopal et al., 2005). The description of HA
144 properties relies on several assumptions, and the various models include a more or less detailed
145 description of metal ion-HA interaction. In particular, the electrostatic and chemical contributions
146 to the overall metal ion-HA binding are separated in the models. This is a major advantage for
147 understanding metal ion-HA binding in saline solutions, because ionic strength is expected to
148 more strongly affect electrostatic than chemical binding properties of HA. Unfortunately, as
149 pointed out by Tipping (1998), the electrostatic approach included in Models V/VI/VII is
150 unlikely to be applicable for $I > 1$ m. In contrast, NICA-Donnan equations seem to be applicable
151 in highly saline conditions (up to 2 M), as shown for HA proton titration data (Benedetti et al.,
152 1996), but, to our knowledge, it has never been tested for metal ion-HA complexation data.

153 In the following, we evaluate the applicability of Model VII and the NICA-Donnan model
154 for saline aqueous solutions, focusing on the concomitant electrostatic approaches. The following
155 analysis involves close inspection of the model equations in conjunction with comparisons of
156 simulated and experimental HA proton titration and radionuclide complexation data. The
157 mechanisms responsible for the effect of ionic strength on cation-HA complexation are also
158 discussed within the context of the assumptions inherent to Model VII and NICA-Donnan.
159 Finally, the impact of the physico-chemical conditions on the experimental determination of SIT
160 parameters for more simple cation-HA models is discussed.

161

162 ## 2. Theoretical background

163 ### 2.1. Aqueous speciation calculations and codes

164 Ionic strength (*I*) affects the activity of dissolved ions in solution, which must be
165 accounted for, for instance, when extrapolating formation constants to hypothetical infinite
166 dilution condition (i.e., for $I = 0$ *m*). In the present study, activity coefficients (γ) are calculated
167 according to the specific ion interaction theory (SIT; Ciavatta, 1980). SIT is generally considered
168 valid for ionic strengths up to 3 - 4 *m*. At 25 °C, activity coefficients for an aqueous species *i* with
169 a charge z_i are calculated as follows:

$$\log \gamma_i = -{z_i}^2 \frac{0.509 \times \sqrt{I}}{1 + 1.5\sqrt{I}} + \sum_k \varepsilon(i,k) \times m_k = -{z_i}^2 D + \sum_k \varepsilon(i,k) \times m_k \qquad (1)$$

170 where D is the Debye-Hückel term used in SIT, m_k is the molality of the aqueous species *k* (mol
171 kg^{-1}), and ε(i,k) is the specific ion interaction coefficient between species *i* and *k* (kg mol^{-1}).

172 In the present study, we use PHREEQC (version 2; Parkhurst and Appelo, 1999) to model
173 cation-HA binding with Model VII. The NICA-Donnan model is not implemented in PHREEQC
174 yet, which will require future modification of PHREEQC code. Therefore, Visual MINTEQ

(version 3.0; Gustafsson, 2012) is used to model cation-HA binding with NICA-Donnan. The SIT database provided with each code is used (which corresponds to ThermoChimie v.7.b in PHREEQC). Unless mentioned in this study, the same thermodynamic constants and SIT parameters were selected throughout. The metastability of ClO_4^-, sometimes used as background anion, is avoided in the models by defining perchlorate as a master species. The Pitzer approach (Pitzer, 1991) can be applied to calculate activity coefficients for aqueous ions in even more concentrated media than appropriate for SIT, which would be more relevant for brine solutions. However, in the present study, the SIT was chosen: (i) for the sake of simplicity, as it is approximately equivalent to a simplified Pitzer model (Grenthe et al., 1993); (ii) because most of the thermodynamic data are taken from the NEA database (Guillaumont et al., 2003), which recommends the use of SIT; and (iii) because Pitzer equations are implemented in PHREEQC but not in Visual MINTEQ, the NICA-Donnan model cannot be tested yet in combination with the Pitzer model.

Experimental pH measurements (pH_{exp}) are affected by the background electrolyte concentration under saline conditions (e.g., Altmaier et al., 2003), and appropriate calibrations are necessary to relate empirical pH_{exp} to the molality of the proton (pH_m = - log m_{H^+}). The deviation between pH_{exp} and pH_m increases with increasing ionic strength such that $pH_{exp} < pH_m$ for concentrated electrolytes. The pH (= - log a_{H^+}), which is a master variable and hence required by speciation codes, can be determined from pH_m and calculated γ_{H^+} values. In this study, SIT is used to calculate pH.

2.2. Determination of empirical metal ion-HA complexation constants

Empirical models consider that the metal ion binds to one generic HA site. Non-specific metal ion-HA interactions are not considered explicitly. The general complexation reaction of a cation M with HA can be written as follows:

$$M + HA \;=\; MHA \qquad (2)$$

and the corresponding conditional stability constant is

$${}^{HA}\beta = \frac{[MHA]}{[M]_f[HA]_f} \qquad (3)$$

Various approaches can be found in the literature to determine $^{HA}\beta$ values. Therefore, it is not possible to directly compare $^{HA}\beta$ values reported in separate M-HA complexation studies unless the same calculations were made or appropriate corrections are applied. The differences arise from the various possibilities for defining $[M]_f$ or $[HA]_f$ in eq. 3. For example, $[M]_f$ may refer to (i) the total dissolved metal ion concentration at equilibrium (noted $[M]_{tot,f}$ in the following), which includes complexes of M with any ligand except HA (e.g. OH^-, Cl^-, CO_3^{2-} or acetate when used as a pH buffer) or (ii) the "free" aquo-ion only, $[M^{z+}]_f$. In the remainder of the text, M-HA complexation constants referring to the total dissolved metal ion concentration and to the aquo-ion will be denoted $^{HA}\beta(M)$ and $^{HA}\beta(M^{z+})$, respectively. $[M^{z+}]_f$ can be calculated by dividing the $[M]_{tot,f}$ value by the side reaction coefficient (α_M; Ringböm, 1963):

$$\alpha_M = 1 + \sum_h \frac{{}^*\beta_h}{m_{H^+}^h} + \sum_l \beta_l \times m_L^l \,. \qquad (4)$$

Here, $^*\beta_h$ are the hydrolysis constants, L is a ligand, β_l are the formation constants for $M(L)_l$ complexes and m_{H^+} and m_L refer to the molalities of H^+ and L. In eq. 4, $^*\beta_h$ and β_l are conditional constants, valid at a given ionic strength. Possible ternary complexes (i.e., involving a

metal ion and two different ligands) or polynuclear species are not included in eq. 4 for the sake of simplicity in the present text, but they must be taken into account in the calculations.

The definition of $[HA]_f$ (eq. 3) also depends on the humic-ion binding model considered. In the present study, the notation of Marquardt and Kim (1998) is used for the different $^{HA}\beta$ (namely, ^{HA}K, $^{HA}\beta_{LC}$ or $^{HA}\beta_{\alpha}$, as defined below). HA site density, commonly corresponding to the proton exchange capacity of HA (PEC, in eq $g(HA)^{-1}$), can be taken into account to determine the total HA site concentration ($[HA]_{tot}$, in eq $kg(H_2O)^{-1}$). The corresponding M-HA complexation constant, denoted ^{HA}K, can be calculated considering that:

$$[HA]_f = [HA]_{tot} - [MHA] \quad (5)$$

where ^{HA}K varies with pH, ionic strength, metal loading, etc.

Competition between the metal ion and H^+ can be included via the degree of deprotonation (α_{HA}) in order to suppress the dependence of the M-HA complexation constant on pH:

$$[HA]_f = [HA]_{tot} \times \alpha_{HA} - [MHA]. \quad (6)$$

The concomitant complexation constant is noted $^{HA}\beta_{\alpha}$ and refers to the Polyelectrolyte Model (PM; Torres and Choppin, 1984). The degree of deprotonation, α_{HA}, is experimentally determined by proton titration and depends on both pH and ionic strength.

Another approach is to consider the effective amount of binding sites at a given pH and *I*. Here, the aim is to suppress the dependence of the M-HA complexation constant on both pH and HA site saturation at high metal loading. In a Pu(IV)-HA study, Szabó et al. (2010) determined the maximum complexing capacity (B_{max}, in mol g^{-1}) of HA immobilized on silica gel (19.9 mg HA g^{-1}), associated with a complexation constant denoted $^{HA}\beta(Pu^{4+})$:

$$[HA]_f = B_{max} - [PuHA] \quad (7)$$

where B_{max} and $^{HA}\beta(Pu^{4+})$ are determined by analyzing SiO_2-HA-Pu binding isotherms with a Langmuir-type equation.

The effective amount of binding considered in the Charge Neutralization Model (CNM; Kim and Czerwinski, 1996) is the "loading capacity" (LC, generally in mol g^{-1}). For this model, it is assumed that the total amount of HA sites that is available to neutralize the metal depends on the metal charge (z). In the CNM, the free HA site concentration is defined as:

$$[HA]_f = [HA]_{tot} \times LC/z - [MHA]. \quad (8)$$

The corresponding M-HA complexation constant is noted $^{HA}\beta_{LC}$.

2.3. Humic-ion binding models NICA-Donnan and Model VII

2.3.1. Chemical part of the models

NICA-Donnan and Model VII have been described in several publications (e.g., Koopal et al., 2005; Tipping et al. 2011). Because the effect of the ionic strength is taken into account through the electrostatic part of these models, the chemical part is only briefly discussed here. Cation-HA complexation (including H^+) in NICA-Donnan and Model VII follows identical reaction equations (eq. 2). Additional equations are used to account for HA heterogeneity. NICA-Donnan describes HA heterogeneity by a continuous affinity distribution for the interaction between a cation and HA, whereas Model VII considers a large number of binding sites with different but discrete affinities for the cation. The chemical cation-HA binding parts of these models aim at describing the overall cation-HA complexation (e.g., expressed as a log ^{HA}K value) as a function of pH, cation to HA concentration ratio (or "metal loading"), and take into account cation competition with a limited number of parameters. The latter parameters are "intrinsic" because they do not vary with the physico-chemical conditions. However, parameters usually vary with the type of HA, including origin or composition. Generic parameters for a wide range

of metal ions and HAs were determined for NICA-Donnan (Milne et al., 2001; 2003) and Model VII (Tipping et al., 2011) by fitting experimental datasets. These generic parameters capture "average" HA behavior, and will be used as such in this study. Consequently, the present work does not aim at discussing the capability of the generic parameters to precisely simulate a given dataset (i.e., no parameter optimization is made). Rather the capability of NICA-Donnan and Model VII to predict variations in apparent cation-HA binding constants with the ionic strength will be discussed (e.g., trends in log ^{HA}K versus I).

It is important to note that, in NICA-Donnan and Model VII, Na^+ is not considered to bind specifically to HA unlike Ca^{2+} or Mg^{2+}, which complex with HA in solution. Therefore, for high 1:1 Na-containing background electrolyte solution (e.g. $NaCl/NO_3/ClO_4$), Na^+ is considered to control the ionic strength and to affect other metal ion complexation by HA only via electrostatic effects.

2.3.2. Electrostatic models

HAs are large and negatively charged polyelectrolytes. This leads to an accumulation of cations in the vicinity of HA binding sites. Electrostatic models aim at converting the dissolved cation concentration in the bulk solution ($[C]_i$) to a local dissolved cation concentration ($[C]_{loc,i}$) that occurs adjacent to the HA site. To accomplish this, the electrostatic potential of HA particles (Ψ, in V) is computed using a Boltzmann factor:

$$[C]_{loc,i} = [C]_i \times \exp(-z_i F\Psi/RT) \quad (9)$$

Here, z_i is the charge of the cation, T is absolute temperature, F is the Faraday constant and R is the gas constant.

Within the NICA-Donnan framework, HAs are considered as permeable spheres. Counter-ions are accumulated in a Donnan phase. The electrostatic potential (Ψ_D) is constant

inside the Donnan volume and equals zero outside (i.e., in the bulk solution). The Donnan volume (V_D, in L kg(HA)$^{-1}$) is calculated as follows:

$$\log V_D = b(1 - \log I) - 1 \quad (10)$$

The parameter b is adjusted by fitting acid-base titration experiments at varying I and depends on the type of HA (origin, composition, etc). In the Donnan volume, the negative charge of HA (Q) is neutralized by counterions:

$$\frac{Q}{V_D} + \sum_i z_i \left([C]_{D,i} - [C]_i\right) = 0 \quad (11)$$

where $C_{D,i}$ and C_i refer to the concentration of the ion i with a charge z_i in the Donnan phase and in the bulk solution, respectively. The activity of the ion in the Donnan phase is required for calculation of the specific binding.

Within the Model VII framework, HA molecules are considered as impermeable spheres. Since the conceptualization of HA particles and the numerical treatment of the electrostatic effects resemble a surface complexation model (e.g., see the present implementation of Model VII in PHREEQC in the following section), we will denote the electrostatic potential Ψ_0, similarly to the surface potential of minerals. The electrostatic correction is an empirical equation that mimics the Boltzmann factor:

$$\exp(-F\Psi_0/(RT)) = \exp(-2PQlog(I)) \quad (12)$$

where I is the ionic strength (mol L^{-1}), P is an adjustable parameter (generally -400 < P < -100 for HA) and Q is the net humic acid charge (eq g^{-1}). In NaCl/NO_3/ClO_4 background electrolytes, the molality and molarity scales do not significantly differ for $I \leq 1$ M (or m). The molality scale is used to extrapolate the model to high I. A Donnan model is also used in the original version of Model VII, but it only accounts for counter-ion accumulation (i.e., to calculate the amount of ion bound to HA in a non-specific manner) and has no effect on electrostatics, in contrast to the NICA-Donnan model. Because in Model VII, HA is considered to be an impermeable sphere of

radius r, the Donnan volume is a layer at the surface of the sphere, with a thickness equal to the Debye length ($\kappa^{-1} = (3.29\times10^{9}\times I^{1/2})^{-1}$; in meters, I in mol L^{-1} and at 25°C). With the molar mass and the radius of HA (15000 g mol^{-1}; 1.72 nm) inherent to Model VII, the surface area of HA (A_{HA}) equals 1500 m^2 g^{-1}. Hence, the Donnan volume in Model VII equals $A_{HA}\times\kappa^{-1}$ (in m^3 g^{-1}). Unfortunately, the "-donnan" keyword cannot be used with SIT and Pitzer options in PHREEQC. It can only be used with other databases, which do not involve SIT or Pitzer models (e.g. which use Davies or Debye-Hückel equations to calculate activity coefficients). However, during preliminary tests, we found very little effect of these calculations on the overall cation-HA binding (see Fig. S2), especially at high I where the Donnan volume drastically shrinks. Therefore, this option is not used in the present study, that is, counter-ion accumulation is neglected.

2.3.3. Implementation of Model VII in PHREEQC

The complete Model VII chemical reaction database, described in Tipping et al. (2011), was previously included in PHREEQC by Marsac et al. (2014) and is used in this study. In the supporting information, a file that can be used to modify Model VII chemical reaction database (e.g., to include other cations or to change binding parameters) and an example of PHREEC input file are given.

Previous studies, where Models V, VI or VII were coupled with PHREEQC, attempted to convert this empirical electrostatic humic ion-binding model into the diffuse layer model (DLM) formalism (Appelo and Postma, 2005; Liu et al., 2008; Marsac et al., 2011, 2014; Catrouillet et al., 2014). Such a conversion requires the calculation of a surface area (A_{HA}) that depends on the ionic strength. Similar computations have been performed for polyelectrolytes such as polyacrylic acid (Lützenkirchen et al., 2011). Such approaches result in physically unreasonable

surface areas (above 10^4 m² g^{-1}) (Appelo and Postma, 2005; Liu et al., 2008; Lützenkirchen et al., 2011; Marsac et al., 2011, 2014; Catrouillet et al., 2014). Hence, we suggest the use of the constant capacitance model (CCM) might be a better choice (Catrouillet et al., 2015). For the CCM, the capacitance (C_1, in F m^{-2}) evolves with log *I* in the case of minerals (Lützenkirchen, 1999), and a log *I*-term is also found in the empirical electrostatic model in Model VII (eq. 12). Specifically, the CCM employs a linear relationship between the charge density at the surface (σ_0, in C m^{-2}) and the surface potential (Ψ_0, in V):

$$\sigma_0 = C_1 \times \Psi_0. \quad (13)$$

Combination of equations 12 and 13 gives:

$$C_1 = F^2 \times (2RTPA_{HA}\log(I))^{-1}. \quad (14)$$

Therefore, using the CCM leads to an expression for C_1 that does not depend on the pH. Given the surface area of HA in Model VII (A_{HA} = 1500 m² g^{-1}), the range of C_1 values found for $I < 1$ *m* corresponds to that commonly reported for minerals ($0.5 < C_1 < 10$ F m^{-2}; Lützenkirchen, 1999). Although the CCM is not implemented in PHREEQC, it can be used by applying appropriate corrections to the three plane model (TPM) in PHREEQC. Details are given in supporting information.

3. Results and Discussion

3.1. Proton titration in saline solutions

Although proton titrations of HA are rarely carried out for $I > 1$ *m*, a number of critical studies do exist. Kurk and Choppin (2000) and Laszak and Choppin (2001) performed proton titrations of HA at I = 0.1, 0.3, 1, 3 and 5 *m* (NaCl), and calculated apparent dissociation constants (pK_a) for HA considering two acidic groups. They found that pK_a variation was insignificant (±0.1) within this range of ionic strengths. Marinsky et al. (1982) reported similar

observations for ionic strength between 0.2 and 2 M $NaNO_3$. Furthermore, the charging curves for HA versus the pH_m reported by Maes et al. (1992) exhibited only slight differences between 1 and 3 M $NaClO_4$. Van Dijk (1959) observed a shift in the titration curves to lower "pH" for *I* increasing from 0.02 to 2 M NaCl but mentioned no pH-correction. This effect is qualitatively consistent with the increased deviation between pH_{exp}-pH_m with increasing *I* ($pH_{exp} < pH_m$) that is commonly observed (e.g., Kurk and Choppin, 2000; Altmaier et al., 2003). The surface of biological cells, such as the seaweed *Ulva lattuca*, can be considered as a polyelectrolyte, and the cation sorption properties onto *U. lattuca* can be treated with the models applied to HA (e.g. Turner et al., 2008). Surface acid-base properties of such biosorbents show very little influence of *I* above 1 *m* (e.g. Rey-Castro et al., 2003; Schijf and Ebling, 2010).

The apparent pK_a of one HA site at a given ionic strength ($pK_a(I)$), which is obtained experimentally, can be written as follows:

$$pK_a(I) = -log\frac{[H^+][HA^-]}{[HHA]} = pK_a(I=0) + log\,(\gamma_{H^+}) - F\Psi/(RTln(10)) \qquad (15)$$

According to eq. 15, the observed small dependence of conditional HA proton dissociation constants on *I* for highly saline conditions (*I* > 1 *m*) might occur (i) due to small dependencies of both Ψ and γ_{H^+}on *I* or (ii) compensation of the effects of *I* on Ψ and γ_{H^+}. Figure 1a compares the effect of *I* on Ψ_0 (for Model VII) and Ψ_D (for NICA-Donnan) at constant proton activity (pH = 5.5). As stated by Tipping (1998), Model VI is unlikely to find application at ionic strengths higher than *I* = 1 *m*, because of the electrostatic model (the same is true for Model VII). When the electrostatic term is translated to the CCM formalism (e.g., to be used in PHREEQC; eq. 14), and for the case when *I* increases to 1 *m*, C_1 tends to infinity and the model becomes essentially non-electrostatic (Ψ_0 = 0). When *I* > 1 *m*, C_1 is negative, which is physically unrealistic,

demonstrating that Model VII cannot be used with PHREEQC when I > 1 m (except by suppressing the electrostatic term), consistent with the conclusion of Tipping (1998).

Benedetti et al. (1996) previously demonstrated the capability of NICA-Donnan to simulate HA charging curves versus pH in highly saline conditions (up to 2 M). In this case Ψ_D increases with I and only small variation in Ψ_D can be seen for I > 1 m (Fig. 1a). The NICA-Donnan model's inherent electrostatic contribution in cation-HA binding is approximately constant (-60 mV ≤ Ψ_D ≤ -40 mV) for I > 1 m, and only a small dependence of apparent pK_a values (i.e., corrected for the activity coefficient effect) on Ψ_D is predicted. This is because the Donnan volume is small for I > 1 m and only slightly shrinks when I further increases. Interestingly, the amplitude of the variation in Ψ is similar for both models when using the generic parameters: $\Psi_D \approx \Psi_0$ – 60 mV for I < 1 m and pH = 5.5, as highlighted in Figure 1a. Therefore, by suppressing the electrostatics in Model VII for $I \geq 1$ m, we produce a comparable effect of I on cation-HA binding constants as in NICA-Donnan. This leads to a simplification of Model VII equations compared to lower I.

Figure 1b shows the change of $\log \gamma_{H^+}$ versus I between 0.1 and 4 m for different background electrolyte solutions (i.e., $NaNO_3$, NaCl, and $NaClO_4$) computed according to the SIT equation, where $\varepsilon(H^+,NO_3^-)$ = 0.07 ± 0.07 for $NaNO_3$, $\varepsilon(H^+,Cl^-)$ = 0.12 ± 0.01 for NaCl, and $\varepsilon(H^+,ClO_4^-)$ = 0.14 ± 0.03 for $NaClO_4$ electrolytes. The maximum variation in $\log(\gamma_{H^+})$ between 1 and 4 m, as calculated with SIT, is approximately 0.16 in $NaNO_3$, 0.31 in NaCl and 0.37 in $NaClO_4$, corresponding to a small dependence of the predicted apparent pK_a values on $\log(\gamma_{H^+})$. The slight variation in both Ψ and γ_{H^+} for 1 < I < 4 m is consistent with the experimental observations showing little dependence of apparent pK_a with I under highly saline conditions (Marinsky et al., 1982; Maes et al., 1992; Kurk and Choppin, 2000). Note that the value of γ_{H^+} has no direct impact on NICA-Donnan results, because concentrations are involved in the

399 equations, and cannot compensate the effects of I on Ψ_D. Therefore, a slight decrease in $pK_a(I)$
400 values is predicted with the NICA-Donnan Model when I increases.

401 To illustrate how PHREEQC-Model VII reproduces acid-base titration data for I > 1 m,
402 Figure 1c shows HA charge versus pH_m in 0.1, 1 and 3 M (0.1, 1.051, 3.503 m) $NaClO_4$
403 determined by Maes et al. (1992), together with results from Model VII. Experimental data of
404 Marinsky et al. (1982) (in $NaNO_3$) and Laszak and Choppin (2001) (in NaCl) with Model VII
405 simulations are shown in Figure S4. For a better illustration, slight adjustment of site densities
406 and pK_a values was made (see table S1), in order to better reproduce experimental data for I = 0.1
407 M, and predictions are made for higher I. HA charge increases between I = 0.1 and 1 M, which is
408 well predicted. Between I = 1 and 3 M, experimental HA charge decreases, as also predicted by
409 Model VII. This charge decrease is actually related to the use of a pH_m-scale: with a pH-scale
410 (see Fig. S3), Model VII simulations for I = 1 and 3 M cannot be differentiated (due to the
411 suppression of the electrostatic term), and the difference between the two experimental curves is
412 smaller. Beside small discrepancies between experimental and model results, it can be concluded
413 that Model VII does a relatively good job in predicting HA charging curves in saline conditions.

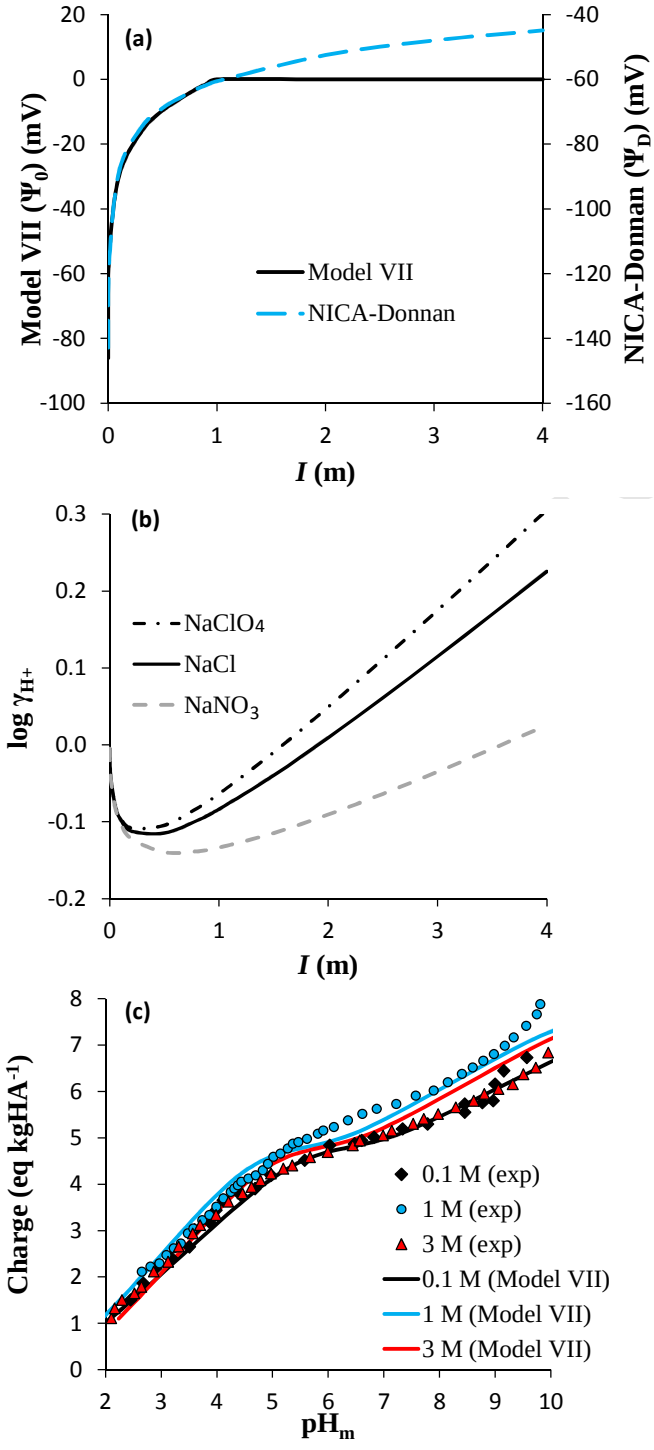

414

415 **Figure 1.** (a) Surface potential (Ψ_0) and Donnan potential (Ψ_D) calculated for Model VII and
416 NICA-Donnan, respectively, for pH (= - log a_{H^+}) = 5.5 versus the ionic strength. The y-axis for
417 Ψ_D is shifted by 60 mV compared with the one of Ψ_0 to highlight their similar evolution with *I*.
418 (b) Activity coefficient of the proton ($\log \gamma_{H^+}$) versus *I* in NaCl, $NaClO_4$ and $NaNO_3$ solutions,

419 calculated with SIT. (c) HA charge versus pH_m in 0.1 M (black curve), 1 M (blue curve), and 3
420 M (red curve) [0.1, 1.051, 3.503 m, respectively] $NaClO_4$. Points are experimental results of
421 Maes et al. (1992) and lines are results from Model VII. (For interpretation to references to color,
422 the reader is referred to the web version of this article.)

423

424 **3.2. Anticipated effects of high ionic strengths on metal ion-HA binding**

425 As for the proton, apparent metal ion complexation constants with one HA site at a given
426 ionic strength (log K(I); data that can be obtained experimentally) can be calculated as follows:

$$\log {}^{HA}\beta\,(I) = log\,\frac{[MHA^{z_i-x}]}{[M^{z_i+}][HA^{x-}]}$$

$$= \log {}^{HA}\beta\,(I=0) + log\,(\gamma_{M^{z_i+}}) - z_i F\Psi/(RTln(10)) \qquad (16)$$

427 The term $z_i F\Psi/(RTln(10))$ leads to substantial log $^{HA}\beta$(I) variations for $I < 1\ m$. The amplitude
428 of log $^{HA}\beta$(I) variations should increase with increasing metal ion charge z_i. It should also vary
429 with Ψ, and hence with the HA charge, Q. Therefore, we can expect that larger log $^{HA}\beta$(I)
430 variations would be observed at high pH and low metal loading compared to low pH and high
431 metal loading. These three anticipated effects are purely related to HA physico-chemical behavior,
432 which are predicted by Model VII and NICA-Donnan equations and parameters.

433 Other effects can be anticipated, which are not related to HA behavior but to physico-
434 chemical phenomena in solution. As for the proton, $\gamma_{M^{z_i+}}$varies with the ionic strength and the
435 nature of background electrolytes (eq.1), which would directly affect log $^{HA}\beta$(I) in eq.16. In the
436 presence of complexing ligands other than HA (e.g., OH^-, CO_3^{2-}, Cl^-, acetate, etc), conditional
437 metal-ligand complexation constants will also evolve with ionic strength, which would affect
438 α_M(eq.4). Therefore, we can expect that (i) the presence of ligands will affect trends in log $^{HA}\beta$
439 versus I whatever the mathematical expression used for log $^{HA}\beta$ (see section 2.2) is, and (ii) M-
440 HA complexation constants referring to the total dissolved metal ion concentration ($^{HA}\beta$(M)) and

441 to the aquo-ion ($^{HA}\beta(M^{z+})$) might diverge when varying *I*. For instance, if all conditional metal-
442 ligand complexation constants increase with increasing *I*, $^{HA}\beta(M)$ will decrease, whereas
443 $^{HA}\beta(M^{z+})$ will increase because α_M increases with increasing *I*. Prediction of ionic strength effects
444 on $\gamma_{M^{z_i+}}$ and metal-ligand complexation constants pertain to the thermodynamic database used for
445 aqueous solution (thermodynamic constants and SIT parameters). Therefore, in the presence of
446 ligands other than HA, it is more difficult to test the applicability of Model VII and NICA-
447 Donnan in saline solutions because ionic strength effects on metal-ligand complexation must be
448 discussed in parallel. In particular, experiments conducted in NaCl solutions are affected by M-Cl
449 complexation, which increases with increasing $[Cl^-]$, and consequently, the conditional M-Cl
450 complexation constants also evolve with *I*. For this reason, metal ion-HA binding data measured
451 in $NaClO_4$ are initially discussed below (i.e., section 3.3), followed by data collected in NaCl
452 background electrolyte solutions (section 3.4).
453
454 **3.3. Cation-HA complexation in $NaClO_4$ solutions**
455 **Am(III)/Cm(III).** Czerwinski et al. (1996) investigated Am^{3+} and Cm^{3+} complexation
456 with HA at pH_m = 6 and in various *I* ($NaClO_4$ electrolyte solution). Because (i) most of the data
457 are available for Am^{3+} and (ii) Am^{3+} and Cm^{3+} are generally considered as chemical analogues,
458 they will not be distinguished and we will only refer to Am^{3+} for both datasets in this section. The
459 authors interpreted the data according to the CNM. Only those datasets that allow the
460 determination of the *LC* (i.e., for *I* = 0.01, 0.1, 1.05 and 3.5 *m*) and that are within the
461 applicability of SIT (*I* < 4 *m*) are considered in the present study. The original authors provided
462 the complete raw dataset, which are not reproduced herein. The data are plotted in the form of a
463 binding isotherm, [AmHA] (in mol kg_{HA}^{-1}) versus $[Am]_{tot,f}$ (in μm), for each *I* on Figure 2a. Note
464 that the experimental data for $[Am]_{tot,f} > 8\ \mu m$, which are only available for 0.1 and 3.5 *m*, are not

shown for clarity. In addition, the two separate series of experiments in I = 0.01, 0.1 and 1 m cannot be visually distinguished on Figure 2a. All the isotherms exhibit a plateau at ~1 mol kg_{HA}^{-1}. However, a linear decrease of the LC was observed with $\sqrt{I}$. For I < 1 m, log ${}^{HA}\beta_{LC}$ was shown to decrease, whereas it increased for I > 1 m, although in all cases the maximum variation in log ${}^{HA}\beta_{LC}$ is relatively small. Accordingly, the original authors reported an average value of log ${}^{HA}\beta_{LC}$ = 6.24 ± 0.14. Below, we test the capabilities of Model VII and NICA-Donnan to predict the effect of the ionic strength on log ${}^{HA}\beta_{LC}$ and LC for data from Czerwinski et al. (1996). To do so, simulations are made with Model VII and NICA-Donnan under the same conditions as those studied by Czerwinski et al. (1996). The model results are then treated using the equations of the CNM.

The results of the simulations with Model VII are shown on Figure 2a, where the measured and simulated Am-HA binding isotherms for various I are compared. Some discrepancies (either underestimation or overestimation of the model) are observed, which we attribute to the use of generic Model VII parameters and will not be further discussed. As observed experimentally, Model VII predicts decreasing Am-HA complexation with increasing I from 0.01 to 1 m. However, unlike the experimental results, Am-HA complexation is predicted to increase as ionic strength increases from 1 m to 3.5 m $NaClO_4$. Because Model VII is used as a non-electrostatic model (Ψ_0 = 0) for $I \geq$ 1 m, the discrepancy between the experimental data and the model results can best be explained by changes in the activity coefficient of Am^{3+}, which increases between 1 and 3.5 m $NaClO_4$ according to SIT ($\varepsilon(Am^{3+},ClO_4^-)$ = 0.49 kg mol^{-1}; Guillaumont et al., 2003), as anticipated in eq.1 and eq.16.

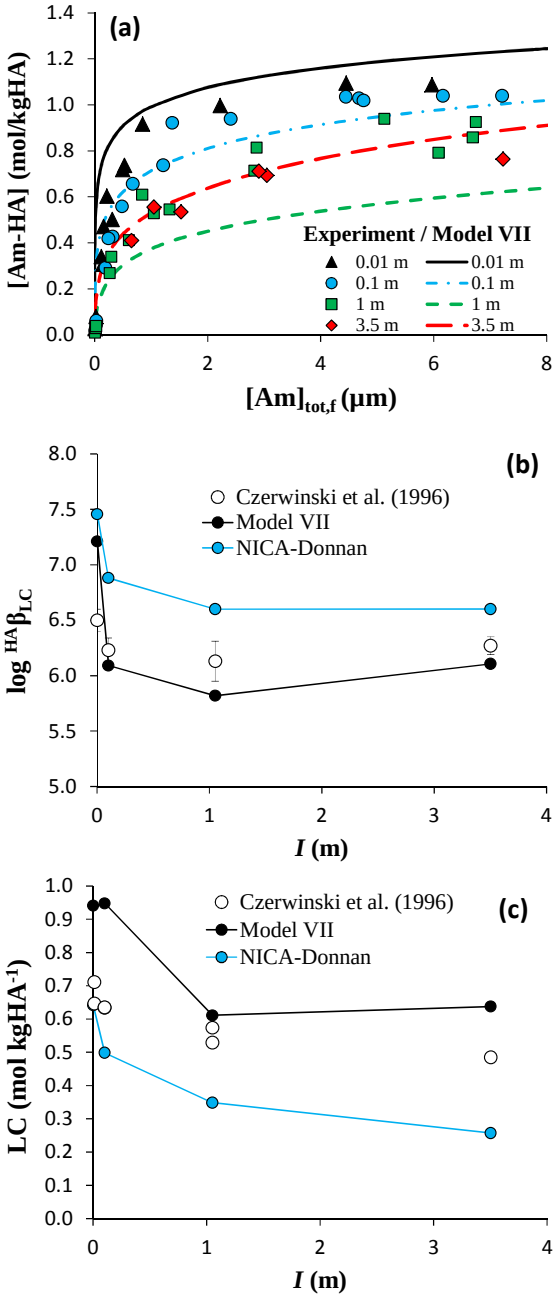

Figure 2. (a) Experimental Am-HA binding isotherms of Czerwinski et al. (1996) for pH_m = 6 and m_{NaClO_4} = 0.01, 0.1, 1 and 3.5 m (symbols) compared with simulations using Model VII (lines). Experimental (b) log $^{HA}\beta_{LC}$ and (c) loading capacity (*LC*) values for Am compared with Model VII and NICA-Donnan predictions versus *I* ($NaClO_4$) in the experimental conditions of Czerwinski et al. (1996). Experimental error bars are generally smaller than the symbols.

Although Model VII accounts for HA heterogeneity, over a limited range of $[Am]_{tot}$, the model Am-HA isotherm can be approximated by a Langmuir-type isotherm. With this approximation, simulations of Am-HA binding with Model VII are treated according to the CNM equations (given in detail in Czerwinski et al., 1996) to determine ${}^{HA}\beta_{LC}$ and *LC*. The results are plotted, respectively, on Figure 2b and 2c. Within the CNM formalism, Model VII consistently predicts a decrease of both *LC* and ${}^{HA}\beta_{LC}$ with increasing *I* from 0.01 and 1 *m*. The increasing activity of Am^{3+} between 1 and 3.5 *m* $NaClO_4$ leads to an apparent increase of both *LC* and ${}^{HA}\beta_{LC}$. Overall, the effect of *I* predicted by Model VII is consistent with the experimental observations although the variations in *LC* and ${}^{HA}\beta_{LC}$ values are larger, as already pointed out. The same exercise with NICA-Donnan yields *LC* and ${}^{HA}\beta_{LC}$ that are also shown in Fig. 2b,c. Although *LC* and ${}^{HA}\beta_{LC}$ values obtained with NICA-Donnan are lower and higher than the experimental values, respectively, the effect of *I* is generally well predicted. Unlike Model VII, NICA-Donnan predicts decreasing Am-HA complexation between 1 and 3.5 *m* $NaClO_4$ because the change in $\gamma_{Am^{3+}}$ cannot compensate for the increase in Ψ_D with increasing *I*, according to NICA-Donnan equations (i.e. based on Am^{3+} concentrations).

Pu(IV). A further example that can be analyzed in the present context is the study by Szabò et al. (2010) on Pu(IV) complexation to a HA grafted silica gel (HA = 20 mg g^{-1}) at pH = 4 and $0.02 < I < 3.5$ *m* ($NaClO_4$). To our knowledge, no Pu(IV)-HA binding parameters are available for NICA-Donnan, and hence, only Model VII can be discussed. The Pu(IV)-HA binding parameters for Model VII are taken from Marsac et al. (2014). Preliminary calculations showed that the formation of polynuclear Pu(IV) species in the presence of HA (Marsac et al., 2014) is not expected for the experimental conditions studied by Szabò et al. (2010). Marsac et al. (2014) used a DLM to account for electrostatic effects when coupling PHREEQC and Model VII,

but the surface area of HA was adjusted to obtain results similar to the original version of Model VII. Here, the same results are obtained when using the CCM to account for electrostatic effects. A modeling approach similar to that used for Am is applied to Pu (Fig. 3). Simulations were performed with Model VII for conditions comparable to those studied by Szabò et al. (2010). The simulated Pu-HA binding isotherms for each ionic strength are treated according to the equations given in the latter study to determine the maximal binding capacity of the HA grafted silica gel for Pu (B_{max}) and log ${}^{HA}\beta(Pu^{4+})$. The calculations include the side reaction coefficient for Pu(IV) (i.e., eq. 4), and the Pu(IV) hydrolysis constants and SIT parameters employed by Szabò et al. (2010), which were originally obtained from Guillaumont et al. (2003). It is important to note that Pu(IV) exhibits strong hydrolysis and that, at pH = 4, α_{Pu} varies with *I* because of ionic strength effects on conditional Pu(IV) hydrolysis constants.

Simulations with Model VII are compared to the experimental results of Szabò et al. (2010) in Figure 3. The experimental B_{max} decreases with increasing *I* up to *I* = 0.5 *m* and thereafter remains nearly constant up to *I* = 3.5 *m*. Model VII predicts little variation in B_{max} with ionic strength (i.e., predicted B_{max} ranges between 0.52-0.59 µmol g^{-1}), in contrast to variation of the experimental results (0.16-1.57 µmol g^{-1}), and to the modeled $LC_{Am(III)}$ variations. Differences between modeling results for Am^{3+} and Pu^{4+} likely arise either from the different metal loadings investigated ([Am(III)-HA] ≤ 1 and [Pu(IV)-HA] ≤ 3×10^{-2} mol $kgHA^{-1}$), which has an impact on HA charge, because Pu^{4+} and Am^{3+} show different hydrolysis behavior, or because HA grafted silica gel behaves differently than dissolved HA. Presently, we cannot explain the discrepancies between experimental and model results for Pu^{4+}. Nevertheless, the predicted variation in B_{max} falls within the experimental range reported by Szabò et al. (2010) so that the impact on the prediction of overall Pu^{4+}-HA binding is limited. Experimental and simulated log ${}^{HA}\beta(Pu^{4+})$ values are also shown in Figure 3. Generally good agreement is found between the experimental

and predicted log $^{HA}\beta(Pu^{4+})$ values (Fig. 3), i.e., a decrease up to I = 1 m followed by an increase up to 3.5 m. The differences are about ±0.5 log units for the stability constant. For Ψ_0 = 0 (i.e., for I > 1 m), the increase in log $^{HA}\beta(Pu^{4+})$ between I = 1 and 3.5 m is due to α_{Pu}, which increases by 0.84 log units over this range of I at pH = 4. Indeed, according to the SIT model, $[Pu^{4+}]$ decreases with increasing I because of the formation of its hydrolysis products (i.e. the $\sum_h \frac{^*\beta_h}{m_{H^+}^h}$ term increases in eq. 4). This phenomenon is not observed with Am^{3+} because its hydrolysis can be neglected at pH = 6 and 0 < I < 4 m.

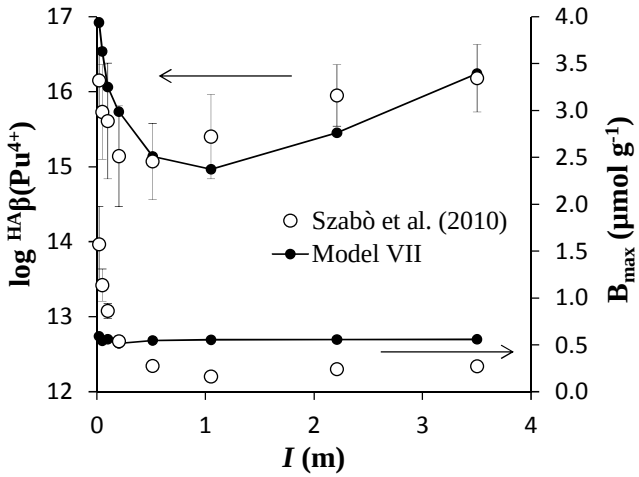

Figure 3. Experimental binding capacity (B_{max}) and log $^{HA}\beta(Pu^{4+})$ values of Szabò et al. (2010) versus I ($NaClO_4$) compared with Model VII predictions. Arrows refer to the y-axis corresponding to the data. Experimental error bars for B_{max} are generally smaller than the symbols.

3.4. Cation-HA complexation in NaCl solutions

In a number of laboratory studies, Choppin and co-workers (Labonne-Wall et al., 1999; Kurk and Choppin, 2000; Laszak and Choppin, 2001; Wall et al., 2002) investigated $U^{VI}O_2^{2+}$, Co^{2+}, Ni^{2+}, Ca^{2+} and Am^{3+} complexation with HA in m_{NaCl} solutions by solvent extraction methods in ambient (air) atmosphere. A summary of the experimental conditions is given in Table 1. Only data within the applicability of SIT (I < 4 m) are considered in the present study. Although Cl^- is clearly a more relevant background anion than ClO_4^- in the environment, the interpretation of M-HA complexation data obtained for high m_{NaCl} are more difficult because, unlike ClO_4^-, Cl^- is a complexing anion, albeit, a weak one. In addition, the Am- and U(VI)-HA experiments were carried out in the presence of 0.01 M acetate buffer. Acetate is known to bind to metal ions and must therefore be taken into account in the calculations (Labonne-Wall et al., 1999; Wall et al., 2002). Finally, unlike the other cations, for $pH_m \approx 5$ under ambient (air) atmosphere, UO_2^{2+} hydrolysis and complexation by carbonate anions cannot be neglected (Langmuir, 1978; Labonne-Wall et al., 1999). Therefore, M-HA complexation datasets obtained for high m_{NaCl} are less suitable for testing the applicability of NICA-Donnan and Model VII than experiments conducted in a more inert background electrolyte such as $NaClO_4$. Indeed, it was found that the modeling results discussed below strongly depend on the thermodynamic databases in solution and their respective capabilities to accurately handle the speciation of Am^{3+}, UO_2^{2+}, Ni^{2+}, Co^{2+} and Ca^{2+} in saline solutions, even in the absence of HA.

577 **Table 1.** Summary of the experimental conditions for the M-HA complexation experiments of
578 Wall et al. (2002) (Am^{3+}), Labonne-Wall et al. (1999) (UO_2^{2+}), Kurk and Choppin (2000) (Co^{2+}
579 and Ni^{2+}) and Laszak and Choppin (2001) (Ca^{2+}).

	[M] (mol L^{-1})	[HA] (mg L^{-1})	m_{NaCl} (m)	pH	pH buffer
Am^{3+}	1×10^{-9}	1 - 10	0.1 - 6	5.1 (pH_m)	10^{-2} M acetate
UO_2^{2+}	5.24×10^{-7}	2 - 10	0.1 - 6	4.9 (pH_m)	10^{-2} M acetate
Ni^{2+}	1×10^{-9}	2×10^{-3} - 1.6×10^{-2}	0.3 - 5	6.0 (pH_{exp})	No
Co^{2+}	1×10^{-10}	1.3×10^{-2} - 2.2×10^{-1}	0.3 - 5	6.0 (pH_{exp})	No
Ca^{2+}	1×10^{-8}	0 - 500	0.1 - 3	4.5 - 9.5 (pH_m)	No

580
581
582 The reported M-HA complexation constants pertain to the PM (Labonne-Wall et al.,
583 1999; Kurk and Choppin, 2000; Laszak and Choppin, 2001; Wall et al., 2002). For the studies
584 listed in Table 1, α_{HA} values were determined for each pH and *I* from HA proton titrations for the
585 specific metal ion-HA complexation studies. Because NICA-Donnan and Model VII are able to
586 describe M-HA complexation as a function of the pH, it is more convenient to compare
587 experimental constants that have not been corrected for α_{HA}. This can be easily accomplished
588 because all of these studies focused on low metal loadings, where [MHA] can be neglected in eq.
589 6 (i.e., $[HA]_f \approx [HA]_{tot} \times \alpha_{HA}$). Note that the carboxylic groups of HA were considered
590 responsible for M-HA complexation and only these groups were considered in the calculation of
591 $[HA]_{tot}$ (eq. 5-6) (Labonne-Wall et al., 1999; Laszak and Choppin, 2001; Wall et al., 2002).
592 Labonne-Wall et al. (1999) and Wall et al. (2002) reported 1:1 and 1:2 UO_2^{2+}/Am^{3+}-HA
593 complexation constants. Because, the constants show similar variation with *I*, either for UO_2^{2+} or
594 Am^{3+}, the 1:2 complexes are not discussed here and the simulations are made for the lowest [HA]
595 investigated experimentally (i.e., where the 1:1 complex prevails).

596 **Am(III).** Wall et al. (2002) investigated the effect of NaCl on Am-HA complexation for
597 pH_m = 5.1 in 0.01 M acetate buffer. Although constants were corrected for effects of side

598 reactions, such as the formation of Am^{3+}-acetate complexes (eq. 4), Am-Cl complexation was not
599 taken into account by the original authors. Side reaction corrections for the formation of Am^{3+}-
600 acetate complexes employed stability constants reported by Moore et al. (1999).

601 Our simulations using Model VII and NICA-Donnan are for the lowest HA concentration
602 ([HA] = 1 mg L^{-1}). Preliminary calculations showed that Am-Cl and Am-acetate complexation
603 have no more than a minor impact on the trend in $^{HA}K(Am^{3+})$ versus *I*. Experimental and
604 simulated results (now accounting for Am-Cl complexation) are compared on Figure S5. Good
605 prediction of Am^{3+}-HA binding is obtained by both models using generic parameters for I = 0.1
606 m, where experimental uncertainty is relatively large, whereas data for all other *I* are
607 overestimated (see Fig. S5). To better compare experimental and simulated effects of *I* on
608 $^{HA}K(Am^{3+})$, model results were decreased by 1.5 log unit on Figure 4a. In fact, the adjustment of
609 Am-HA binding parameters would produce the same results. When using the generic Am-HA
610 binding parameters, both models produce similar results, especially for the evolution of log K
611 with *I*, as would be expected from the similar variation of Ψ_0 and Ψ_D with *I* (Fig. 1a). Although
612 model log $^{HA}K(Am^{3+})$ values variations with *I* are not as pronounced as experimental ones, the
613 trend is consistent. Nearly constant log $^{HA}K(Am^{3+})$ values are predicted for $I > 1$ *m* by both
614 approaches, which agrees relatively well with the experimental results. Unlike Model VII (where
615 $\Psi_0 = 0$ for $I > 1$ *m*), NICA-Donnan predicts a slight decrease of $^{HA}K(Am^{3+})$ for $I > 1$ *m*. This is
616 related to the evolution of Ψ_D with *I*, and the fact that NICA-Donnan equations do not account for
617 $\gamma_{Am^{3+}}$. Overall, the deviation between both models is small, as expected (Fig. 1a), showing that,
618 by accounting for electrostatic effects, results from Model VII and NICA-Donnan can be
619 extrapolated to highly saline conditions, provided that the specific binding parameters are
620 calibrated for the respective type of HA.

621 **U(VI).** Labonne-Wall et al. (1999) investigated the effect of *I* on U(VI)-HA complexation
622 for pH_m = 4.9 and 0.01 M acetate. UO_2^{2+}-acetate complexation constants were taken from Moore
623 et al. (1999) and are also presently used. We simulated the experimental data of Labonne-Wall et
624 al. (1999) using Model VII and NICA-Donnan for the lowest HA concentration ([HA] = 2 mg L^{-1})
625 and the generic U(VI)-HA binding parameters. As for Am, preliminary tests showed that
626 inclusion or omission of UO_2^{2+}-Cl complexation did not impact the trend in $^{HA}K(UO_2^{2+})$ versus *I*.
627 Experimental and simulated results are compared on Figure 4a. The generic U(VI)-HA
628 parameters produce accurate predictions of the $^{HA}K(UO_2^{2+})$ measured by Labonne-Wall et al.
629 (1999) as well as the evolution of $^{HA}K(UO_2^{2+})$ with *I* up to 2 *m*. At *I* = 3 m, a higher $^{HA}K(UO_2^{2+})$
630 value than at *I* = 2 *m* was measured, which is also predicted by Model VII. As in the case of Pu^{4+},
631 where the apparent hydrolysis constants increase with m_{NaClO_4} above 1 m, this increase in
632 $^{HA}K(UO_2^{2+})$ is driven by $\alpha_{U(VI)}$. Similar conclusions can be made with NICA-Donnan, except a
633 smaller re-increase in $^{HA}K(UO_2^{2+})$ that was observed with increasing *I*, as seen and explained for
634 Am^{3+}. Interestingly, in agreement with the experimental data, Model VII and NICA-Donnan
635 predict a more pronounced decrease in $^{HA}K(Am^{3+})$ than for $^{HA}K(UO_2^{2+})$ when *I* increases from 0
636 to 1 *m*. This feature is driven by the Boltzman factor (eq. 9), which involves the net charge of the
637 cation (i.e. +3 versus +2, respectively) for Am(III) and U(VI).
638

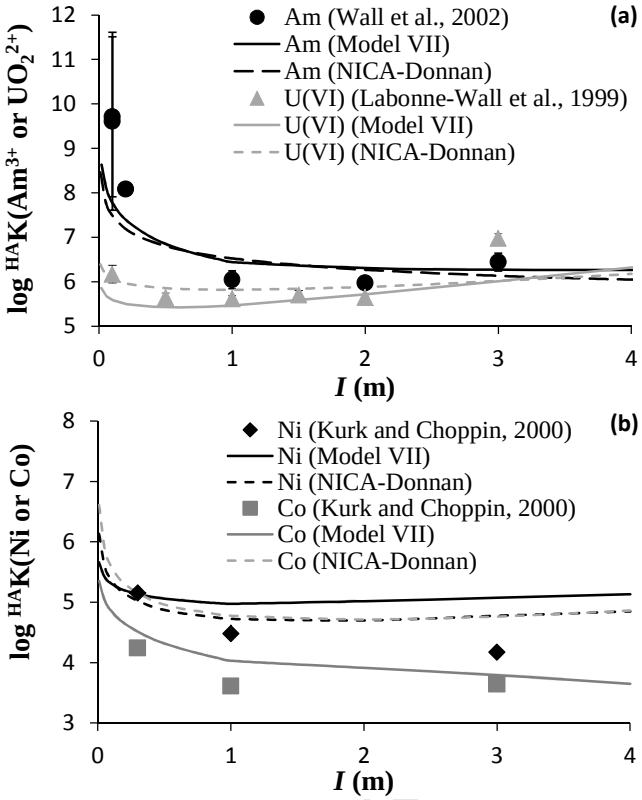

639

640 **Figure 4.** (a) Apparent Am-HA and U(VI)-HA complexation constants (Wall et al., 2002;
641 Labonne-Wall et al., 1999) versus *I* (NaCl) for pH_m = 5.1 and 4.9, respectively. (b) Apparent M-
642 HA complexation constants (M = Ni^{2+} or Co^{2+}, Kurk and Choppin, 2000) versus *I* (NaCl) for
643 pH_{exp} = 6. For both figures, lines are predictions by Model VII (full line) and NICA-Donnan
644 (dashed lines) using the generic parameters (but shifted down for the case of Am-HA, see text for
645 details). Experimental error bars are commonly smaller than the symbols.

646

647 **Co(II)/Ni(II).** Kurk and Choppin (2000) investigated the effect of *I* on Co- and Ni-HA
648 complexation. Unlike Am and U(VI), with data obtained for constant pH_m, Co and Ni data are
649 reported for constant pH_{exp} = 6 by Kurk and Choppin (2000), noting that the deviation between
650 pH_{exp} and pH_m increases with increasing *I*. For example, for pH_{exp} = 6 and *I* = 4 *m*, and with the
651 calibration provided by the original authors, the corresponding pH_m value is 6.95. The originally
652 reported constants were not corrected for side reactions. Again, our simulations using Model VII

and NICA-Donnan were conducted using the lowest HA concentrations reported by Kurk and Choppin (i.e., [HA] = 1.3×10^{-2} mg L^{-1} for Co; [HA] = 2×10^{-3} mg L^{-1} for Ni).

Experimental and simulated results are compared on Figure 4b. With the generic Co/Ni-HA parameters, Model VII overestimates Co/Ni-HA complexation by 1 log unit in the worst case (i.e., for ^{HA}K(Ni) at I = 3 *m*). Model VII consistently predicts a decrease in ^{HA}K with I increasing from 0.3 to 1 *m*, whereas for I > 1 m, the predicted ^{HA}K for Co and Ni diverge. Although pH_m increases by 0.6 units (for constant pH_{exp}) between I = 1 and 3 *m*, ^{HA}K(Ni) remains almost constant, whereas ^{HA}K(Co) decreases by 0.2 log units. These variations reflect the complexation of both of these transition metals by Cl^- in solution. In the SIT database provided with PHREEQC, only the $NiCl^+$ species is included, with $\varepsilon(NiCl^+;Cl^-)$ = 0.1, whereas four Co-Cl complexes are considered (i.e., from $CoCl^+$ to $CoCl_4^{2-}$), all without SIT parameters (i.e. $\varepsilon(i;k)$ = 0). In the SIT database provided with Visual MINTEQ, Co- and Ni-Cl complexation are described similarly and NICA-Donnan predicts the same trend in ^{HA}K(Ni) and ^{HA}K(Co) versus I. The reliability of the thermodynamic aqueous databases is beyond the scope of the present paper. Nonetheless, despite the potential uncertainties in the databases, overall, the predicted effect of I is relatively small above 1 *m* for both Ni and Co, in agreement with the experimental results.

Ca(II). Figure 5 shows ^{HA}K(Ca^{2+}) measured by Laszak and Choppin (2001) for m_{NaCl} = 0.1, 1 and 3 *m* at various pH_m under ambient atmosphere. The originally reported constants were corrected for side reactions (including Ca complexation to chloride and carbonate). Simulations are made with Model VII and NICA-Donnan for 100 mg L^{-1} HA using the generic Ca-HA binding parameters and compared to experimental log ^{HA}K(Ca^{2+}) versus pH_m for I = 0.1 and 3 *m* (NaCl) in Figure 5. Simulations with Model VII for I = 1 *m* do not significantly differ from I = 3 *m* and consequently are not shown. Experimentally, ^{HA}K(Ca^{2+}) increases with pH_m and decreases with increasing I, as for the other cations investigated. Both Model VII (Fig. 5a) and NICA-

677 Donnan do a relatively good job at predicting these trends, although the measured effect of *I* is
678 weaker between 0.1 and 1 *m*, and log $^{HA}K(Ca^{2+})$ are not predicted to evolve substantially for *I*
679 between 1 and 3 *m* with Model VII. Interestingly, the measured effect of *I* appears more
680 pronounced for $pH_m \approx 9$ than for $pH_m \approx 6.5$, which is indeed predicted by both models as
681 anticipated (eq.16). According to the models, the larger negative charge of HA (*Q* being
682 proportional to Ψ_0 *or* Ψ_D) at high pH is responsible for the larger ionic strength dependence of
683 $^{HA}K(Ca^{2+})$.

684 To summarize, beside the deviations between experimental and simulated results that are
685 directly related to the parameterization of $Am^{3+}/UO_2^{2+}/Co^{2+}/Ni^{2+}/Ca^{2+}$-HA complexation for a
686 specific type of HA, the generally observed log $^{HA}K(M^{z+})$ dependence with *I* is relatively well
687 predicted at low metal ion concentration by simply suppressing the electrostatic term in Model
688 VII for $I > 1$ *m*. The NICA-Donnan model shows very similar results without the need to modify
689 the model. More experimental results are required, however, to parameterize these models at high
690 *I* and to test the relevance of additional corrections at high *I* to explain the noted discrepancies,
691 which would make the models more complex. More specifically, complexation studies in non-
692 complexing background electrolyte (e.g., $NaClO_4$) in the absence of pH-buffer (e.g., without
693 acetate) and under inert atmosphere (i.e., in the absence of carbonate) are recommended.

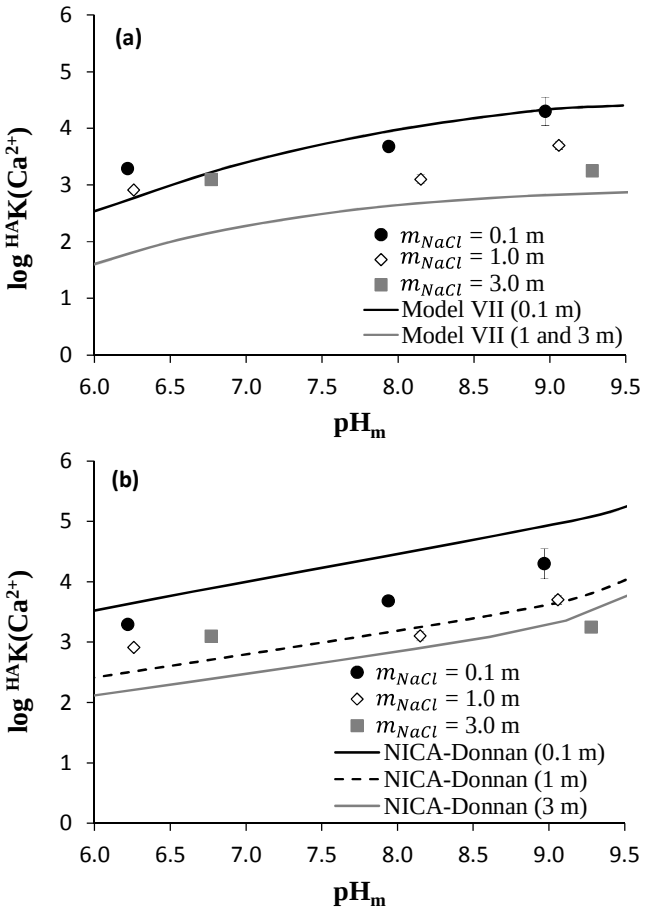

Figure 5. Experimental apparent Ca^{2+}-HA complexation constants versus pH_m for I = 0.1, 1 and 3 m NaCl (Laszak and Choppin, 2001) compared with (a) Model VII (simulated curves for I = 1 and 3 m NaCl overlap) and (b) NICA-Donnan predictions. Experimental error bars are commonly smaller than the symbols on all three figures.

3.5. Metal ion-HA complexation using SIT

To apply simple models such as the PM or the CNM to various ionic strength solutions, they must include the activities of the aqueous species. According to equations 1 and 3, when all physico-chemical conditions are kept constant except I (pH, T, total metal ion concentration), the value of log β (i.e. log ^{HA}K, log $^{HA}\beta_\alpha$, or log $^{HA}\beta_{LC}$) can be extrapolated to I = 0 (log β_0) using:

$$\log \beta = \log \beta_0 - \Delta z^2 \times D - \Delta \varepsilon \times I. \quad (17)$$

For 1:1 complexes between a metal ion (M^z) and a simple ligand (L^y), $\Delta\varepsilon = \varepsilon(ML^{y+z},k) - \varepsilon(M^z,k) - \varepsilon(L^y,k)$, and $\Delta z^2 = (z+y)^2 - z^2 - y^2$. Due to the complexity of HA, Δz^2 and $\Delta\varepsilon$ become adjustable parameters of unclear physical meaning (Czerwinski et al., 1996; Szabò et al., 2010).

Comparing Fig. 2b and Fig. 4a, the effect of *I* on Am-HA complexation appears to differ between the studies of Wall et al. (2002) and Czerwinski et al. (1996), but it is difficult to directly compare the original datasets because: (i) the thermodynamic constants refer to different models; (ii) pH_m differs by one unit; and (iii) the metal loading differs by 3 orders of magnitude. As in Figure 4a for the log ^{HA}K values reported by Wall et al. (2002), log $^{HA}\beta_{LC}$ values determined by Czerwinski et al. (1996) are recalculated to log ^{HA}K values using the *LC* values and imposing negligible [AmHA] in eq. 8. The results are shown in Figure 6a. Although Wall et al. (2002) studied Am-HA complexation at one pH_m unit lower than Czerwinski et al. (1996), their log ^{HA}K values are higher. This can be attributed to the effect of the metal loading. Specifically, at low loading, Am binds to low abundance, strong HA sites, whereas, at high loading, these sites are saturated and Am mainly binds to the more abundant, weaker HA sites (e.g., see Marsac et al., 2010). The effect of *I* below 1 *m* is more pronounced for the dataset of Wall et al. (2002), which would lead to different SIT parameters (Δz^2 and $\Delta\varepsilon$) in eq. 17. Therefore, it is difficult to confidently apply an ionic strength correction for cation-HA binding constants using simple metal ion-HA binding models.

The different ionic strength effects observed by Wall et al. (2002) and Czerwinski et al. (1996) might also arise from differences in metal loading. As pointed out by Hummel et al. (2000), ionic strength effects tend to vanish at high loadings. To illustrate this, log ^{HA}K values for Am-HA complexation are calculated using both Model VII and NICA-Donnan for pH = 5.5, $10^{-3} < I < 4$ *m* (NaCl), 1 mg L^{-1} HA, and $[Am]_{tot} = 10^{-9}$ or 10^{-6} m. The results are normalized to the log

728 ^{HA}K value obtained for I = 1 m (i.e. log ^{HA}K(I) – log ^{HA}K(I = 1 m)) and plotted versus I in Figure
729 6b. Both models indeed predict a more pronounced effect of I on log ^{HA}K at low loading.

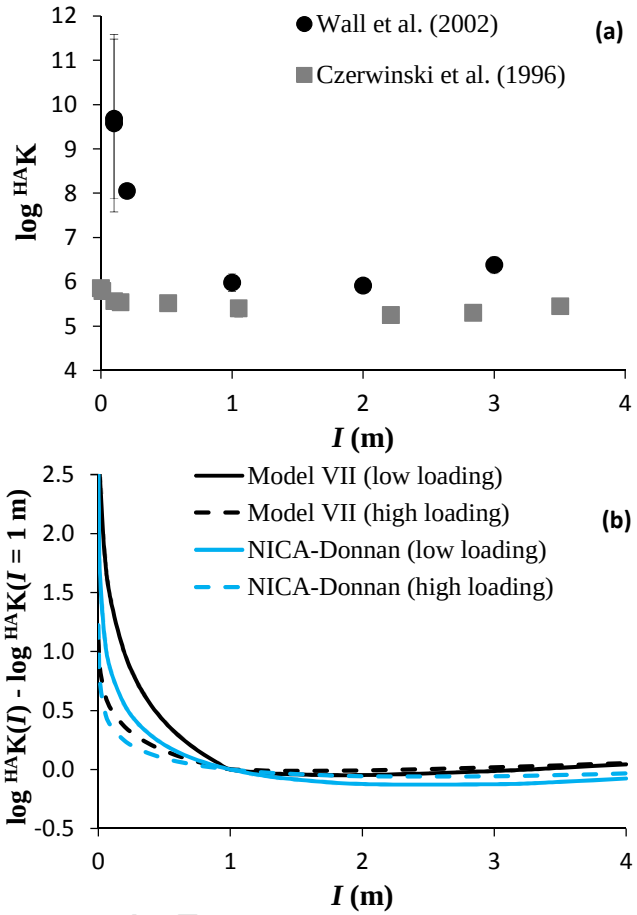

730

731 **Figure 6.** (a) Experimentally observed effect of the ionic strength on Am-HA complexation at
732 low (Wall et al., 2002; pH_m = 5.1; NaCl) and high metal loading (Czerwinski et al., 1996; pH_m =
733 6; $NaClO_4$). (b) Simulated effect of the ionic strength on Am-HA complexation at low ($[Am]_{tot}$ =
734 10^{-9} m) and high metal loading ($[Am]_{tot}$ = 10^{-6} m) with Model VII (black curves) and NICA-
735 Donnan (blue curves) in NaCl for a HA concentration of 1 mg L^{-1} and pH = 5.5. (For
736 interpretation to references to color, the reader is referred to the web version of this article.)
737

738 The effect of I on cation-HA complexation is commonly discussed in terms of
739 conformational changes, which make the physical meaning of the values of SIT parameters in the
740 case of humic materials questionable. Multivalent ions are known to bridge between organic

molecules (Kunhi Mouvenchery et al., 2012), and high concentrations of trivalent actinides lead to the aggregation of HA (Lippold et al., 2005). Hence, the different evolution of log ^{HA}K with *I* observed by Wall et al. (2002) and Czerwinski et al. (1996) may be partially attributed to the aggregation state (or the conformation) of HA in response to different [Am] to [HA] ratios. In Model VII, conformational changes of HA in response to variations of *I* are not explicitly treated, except via a change in Donnan volume, which we find to have a negligible effect on M-HA complexation in saline solutions. Because the charging behavior of HA is related to its conformation, such behavior can implicitly be taken into account within the electrostatic term. In NICA-Donnan, the ionic strength directly affects the Donnan volume. However, none of these models includes effects of conformational changes of HA when $[Am]_{tot}$ increases (e.g., in the case of NICA-Donnan, 10^{-6} *m* of Am would not affect the Donnan volume), by contrast with the more recent Elastic Polyelectrolyte Network electrostatic model (Montenegro et al., 2014). Instead, NICA-Donnan and Model VII explain the less pronounced effect of *I* at increased loading via the charging behavior of HA. In the experiments of Czerwinski et al. (1996), the observed *LC* ranges between 50 and 70% of the PEC. The charge of HA is almost neutralized by Am at the highest $[Am]_{tot}$ investigated, which decreases electrostatic effects and flattens the log ^{HA}K versus *I* curve. Therefore, metal loading is an important parameter not only for the determination of apparent metal ion-HA complexation constants for given pH and *I* conditions, but also for their extrapolation to various ionic strengths (e.g., with SIT).

Unlike Na, with non-specific HA interaction, Ca and Mg bind more strongly to HA, and consequently may affect the charge of HA in brines. Furthermore, other metal ions (e.g. Fe(III), Al(III), divalent transition metals) strongly bind to HA in natural conditions (Kinniburgh et al., 1999; Pinheiro et al., 2000; Tipping et al., 2002; Gustafsson et al., 2007; Marsac et al., 2012; 2013). Hence, the metal loading must be defined on the basis of all cations bound to HA,

765 including H^+. Additional cation competition studies should be conducted at high *I* to improve and
766 homogenize metal ion-HA binding models. As an example, in NICA-Donnan Ca^{2+} mainly
767 interacts electrostatically with HA at high [Ca^{2+}] (Christl, 2012) whereas it chiefly binds
768 specifically to HA in Model VII. As shown in Figure S6, Model VII predicts larger effects from
769 [Ca] on Am-HA complexation than does NICA-Donnan. For pH = 5, 1 m NaCl, [Am] = 10^{-9} m
770 and 1 mg L^{-1} HA, between 0 and 1 m $CaCl_2$, Model VII predicts a decrease of $^{HA}K(Am)$ by 1.5
771 log units against 0.9 using NICA-Donnan. These results highlight another source of variation and
772 uncertainty for Δz^2 and $\Delta\varepsilon$ at high [Ca]. Because it is also suggested that Ca^{2+}-HA interaction is
773 purely electrostatic (van Leeuwen and Town, 2016), Ca^{2+}-metal ion competition experiments at
774 high *I* are required to unravel the role of Ca on metal ion-HA complexation.

775 As shown above, the ionic strength dependence of $^{HA}K(Ca^{2+})$ becomes more pronounced
776 at high pH because of the higher charge of HA. It appears that Δz^2 and $\Delta\varepsilon$, when applied to
777 simple models for M-HA complexation, remain conditional parameters, which depend on the pH,
778 the ionic strength, and the composition of the solution, which in turn affects the loading of HA.
779 Therefore, empirical determination of Δz^2 and $\Delta\varepsilon$ for various conditions requires a large
780 experimental dataset. Because most metal ion-HA binding data at $I > 1$ m were obtained at $pH_m \leq$
781 6, data at higher pH would be necessary to further test the reliability of NICA-Donnan and Model
782 VII.

783 More generally, the use of non-electrostatic models was recently shown to be particularly
784 suitable for the prediction of metal ion sorption to various types of surfaces in brines, including
785 marine microalgae (Schjif and Herbling, 2010; Zoll and Schjif, 2012), bacteria (Ams et al.,
786 2013), illite and smectite (Schnurr et al., 2015). The present data evaluation suggests that this
787 approach can be extended to humic substances using Model VII. Although NICA-Donnan

788 remains an electrostatic model in highly saline solution, the almost invariant Donnan potential
789 produces similar ionic strength effects to those observed using Model VII.

4. Conclusions

The applicability of Model VII and NICA-Donnan was tested at high 1:1 background electrolyte concentration ($NaCl/ClO_4$) in combination with SIT ($I < 4$ *m*). The empirical electrostatic term used in Model VII is related to the constant capacitance model (CCM). A method is proposed to use the CCM in the speciation code PHREEQC, for easier and more consistent implementation of Model VII in this code. The electrostatic term used in this model tends towards zero for $I = 1$ *m*, and thus, further metal ion accumulation in the vicinity of HA molecules can be neglected. Consequently, a non-electrostatic model in combination with the binding site definition in Model VII was tested for $I > 1$ *m*. The approach simplifies the model under these high ionic strength conditions, whereas NICA-Donnan can be used without modification. Both models do a relatively good job in predicting proton dissociation for HA groups where the apparent pK_a variations at high *I* are mainly controlled by the activity coefficient of the proton. The trend in apparent metal ion-HA complexation constants with *I* is consistent with experimental results for Am^{3+}, UO_2^{2+}, Co^{2+}, Ni^{2+}, Ca^{2+} and Pu^{4+}, both at low and high metal loading. The maximum metal ion uptake by HA (e.g., the loading capacity) for various conditions is relatively well predicted. Because of the simple approaches used here and due to the limited number of datasets that are available for highly saline solutions, no attempt was made to improve the models in order to eliminate the discrepancies observed in the evolution of apparent complexation constants with *I*. Most of the discrepancies between experiments and predictions with Model VII or NICA-Donnan are related to the specific cation-HA binding parameters used. With appropriately calibrated specific binding parameters for a given type of HA (e.g. a given composition or origin), both models are expected to reliably predict cation-HA binding for a wide range of ionic strengths.

The impact of the physico-chemical conditions on the experimental determination of SIT parameters for metal ion-HA complexation was also discussed. When HA is treated as a simple dissolved ligand, the obtained SIT parameters values are difficult to interpret with regards to their specific physical meaning owing to the complexity of HA molecules. It is shown here that the experimentally investigated pH and metal loading variations have a strong impact on SIT parameters via their effect on the charge of HA. Some effects of pH and metal loading on cation-HA complexation are well known, but the present study shows that they imply additional effects related to HA charge, which must be taken into account when extrapolating constants at various ionic strengths. Unlike Na, which only interacts electrostatically with HA, Ca or Mg can bind more strongly to HA. Because, highly saline waters commonly have substantial Ca or Mg concentrations, as well as other metal ions, relatively high overall loadings are to be expected. Although Model VII and NICA-Donnan can account for both the metal loading effects and cation competition at $I < 1$ m, additional cation competition experiments at high ionic strength are required to further validate or improve these models. Nevertheless, we suggest that both models might be used as helpful predictive tools in performance safety assessment even under highly saline conditions.

Aknowledgements

This work was financed by the Federal Ministry of Economic Affairs and Energy (Germany) under contracts No. 02E10206 and 02E10961. K. H. Johannesson thanks Michael and Mathilda Cochran for establishing the Cochran Family Professorship in Earth and Environmental Sciences, which provided her financial assistance. We thank three anonymous reviewers and the associate editor (J. P. Gustafsfson) for interesting comments that substantially improved this manuscript.

836 **References**

837 Altmaier M., Metz V., Neck V., Müller R. and Fanghänel Th. (2003) Solid-liquid equilibria of
838 $Mg(OH)_{2(cr)}$ and $Mg_2(OH)_3Cl•4H_2O_{(cr)}$ in the system Mg-Na-H-OH-Cl-H_2O at 25 °C.
839 Geochim. Cosmochim. Acta 67, 3595-3601.

840 Ams D. A., Swanson J. S., Szymanowski J. E. S., Fein J. B., Richmann M. and Reed D. T. (2013)
841 The effect of high ionic strength on neptunium (V) adsorption to a halophilic bacterium.
842 Geochim. Cosmochim. Acta 110, 45-57.

843 Appelo C. and Postma D. (2005) Geochemistry, groundwater and pollution. second ed. Taylor &
844 Francis, New York, p. 595.

845 Benedetti M. F., Milne C. J., Kinniburgh D. G., van Riemsdijk W. H. and Koopal L. K. (1995)
846 Metal-ion binding to humic substances: application of the nonideal competitive adsorption
847 model. Environ. Sci. Technol. 29, 446–457.

848 Benedetti M. F., van Riemsdijk W. H. and Koopal L. K. (1996) Humic substances considered as
849 a heterogeneous Donnan gel phase. Environ. Sci. Technol. 30, 1805-1813.

850 Catrouillet C., Davranche M., Dia A., Bouhnik-Le Coz M., Marsac R., Pourret O. and Gruau G.
851 (2014) Geochemical modeling of Fe(II) binding to humic and fulvic acids. Chem. Geol.
852 372, 109-118.

853 Catrouillet C., Davranche M., Dia A., Bouhnik-Le Coz M., Pédrot M., Marsac R. and Gruau G.
854 (2015) Thiol groups controls on arsenite binding by organic matter: New experimental
855 and modeling evidence. J. Coll. Int. Sci. 460, 310–320.

856 Ciavatta, L. (1980). The specific interaction theory in the evaluating ionic equilibria. Ann. Chim.
857 (Rome) 70, 551–562.

858 Christl I. (2012) Ionic strength- and pH-dependence of calcium binding by terrestrial humic acids.
859 Environ. Chem., 9, 89-96.

860 Czerwinski K. R., Kim J. I., Rhee D. S. and Buckau G. (1996) Complexation of trivalent actinide
861 ions (Am^{3+}, Cm^{3+}) with humic acid: the effect of ionic strength. Radiochim. Acta 72(4),
862 179-187.

863 Fritz P. and Frape S. K. (1982). Saline Groundwaters in the Canadian shield – a first overview.
864 Chem. Geol. 36, 179-190.

865 Grenthe I., Plyasunov A. V. and Spahiu K. (1997) Estimations of Medium Effects on
866 Thermodynamic Data. Chapter IX in "Modeling in aquatic chemistry". OECD
867 Publications, 724 pp. ISBN 92-64-15569-4.

868 Guillaumont R., Fanghänel Th., Fuger J., Grenthe I., Neck V., Palmer D. A. and Rand M. H.
869 (2003) Update on the Chemical Thermodynamics of Uranium, Neptunium, Plutonium,
870 Americium and Technetium, Mompean, F.J., Domenech-Orti, C., Ben-Said, K.,
871 OECD/NEA Data Bank, Eds., vol. 5 of Chemical Thermodynamics, Elsevier, Amsterdam.

872 Gustafsson J. P. Visual MINTEQ version 3.0. http://vminteq.lwr.kth.se/. Stockholm, Sweden,
873 Octobed 2012.

874 Gustafsson J. P., Persson I., Kleja D. B. and van Schaik J. W. J. (2007) Binding of iron(III) to
875 organic soils: EXAFS spectroscopy and chemical equilibrium modeling. Environ. Sci.
876 Technol. 41, 1232-1237.

877 Hesterberg D., Chou J. W., Hutchison K. J. and Sayers D. E. (2001) Bonding of Hg(II) to
878 reduced organic, sulfur in humic acid as affected by S/Hg ratio. Environ. Sci. Technol. 35,
879 2741–2745.

880 Hiemstra T. and van Riemsdijk W. (2006) Biogeochemical speciation of Fe in ocean water. Mar.
881 Chem. 102, 181–197.

882 Hummel W., Glaus M. A. and Van Loon L. R. (2000) Trace metal-humate interactions. II. The
883 "conservative roof" model and its application. Appl. Geochem. 15, 975-1001.

884 Kim J. I. and Czerwinski K. R. (1996) Complexation of metal ions with humic acid: metal ion
885 charge neutralisation model. Radiochim. Acta 73, 5–10.

886 Kinniburgh D. G., Milne C. J., Benedetti M. F., Pinheiro J. P., Filius J., Koopal L. and Van
887 Riemsdijk W. H. (1996) Metal ion binding by humic acid: application of the NICA-
888 Donnan model. Environ. Sci. Technol. 30, 1687–1698.

889 Kinniburgh D. G., van Riemsdijk W. H., Koopal L. K., Borkovec M., Benedetti M. F. and Avena
890 M. J. (1999) Ion binding to natural organic matter: competition, heterogeneity,
891 stoichiometry and thermodynamic consistency. Colloid Surf. A 151, 147-166.

892 Koopal L. K., Saito T., Pinheiro J. P. and van Riemsdijk W.H. (2005) Ion binding to natural
893 organic matter: General considerations and the NICA–Donnan model. Colloids and
894 Surfaces A: Physicochem. Eng. Aspects 265, 40–54.

895 Kunhi Mouvenchery Y., Kučerík J., Diehl D. and Schaumann G. E. (2012) Cation-mediated
896 cross-linking in natural organic matter: a review. Rev. Environ. Sci. Biotechnol. 11, 41–
897 54.

898 Kurk D. N. and Choppin G. R. (2000) Determination of Co(II) and Ni(II)-humate stability
899 constants at high ionic strength NaCl solutions. Radiochim. Acta 88, 583–586.

900 Langmuir D. (1978) Uranium solution-mineral equilibria at low temperatures with applications to
901 sedimentary ore deposits. Geochim. Cosmochim. Acta 42, 547-569.

902 Labonne-Wall N., Choppin G. R., Lopez C. and Monsallier J.-M. (1999) Interaction of uranyl
903 with humic and fulvic acids at high ionic strength. In: Actinide speciation in high ionic
904 strength media: experimental and modeling approaches to predicting actinide speciation
905 and migration in the subsurface. Eds. Reed D. T., Clark S. B. and Rao L., Plenum Pub.,
906 NY, p. 199.

907 Laszak I. and Choppin G. R. (2001) Interaction study between Ca^{2+} and humic acids in brine
908 media. Radiochim. Acta 89, 653–659.

909 Lippold H., Mansel A. and Kupsch H. (2005) Influence of trivalent electrolytes on the humic
910 colloid-borne transport of contaminant metals: competition and flocculation effects. J.
911 Cont. Hydrol. 76, 337–352.

912 Liu D. J., Bruggeman C. and Maes N. (2008) The influence of natural organic matter on the
913 speciation and solubility of Eu in Boom Clay porewater. Radiochim. Acta 96, 711–720.

914 Lützenkirchen J. (1999) The Constant Capacitance Model and Variable Ionic Strength: An
915 Evaluation of Possible Applications and Applicability. J. Coll. Int. Sci. 217, 8-18.

916 Lützenkirchen J., van Male J., Leermakers F. and Sjöberg S. (2011) Comparison of various
917 models to describe the charge-pH dependence of poly(acrylic acid). J. Chem. Eng. Data
918 56, 1602-1612.

919 Maes A., Tits J., Mermans G. and Dierckx A. (1992) Measurement of the potentially available
920 charge and the dissociation behaviour of humic acid from cobaltihexammine adsorption. J.
921 Soil Sci. 43, 669-677.

922 Marinsky J. A., Gupta S. and Schindler P. (1982) The interaction of Cu(II) ion with humic acid. J.
923 Coll. Int. Sci. 89, 401-411.

924 Marquardt C. and Kim J. I. (1998) Complexation of Np(V) with fulvic acid. Radiochm. Acta 81,
925 143-148.

926 Marsac R., Banik N. L., Marquardt C. M. and Kratz J. V. (2014) Stabilization of polynuclear
927 plutonium(IV) species by humic acid. Geochim. Cosmochim. Acta 131, 290-300.

928 Marsac R., Davranche M., Gruau G. and Dia A. (2010) Metal loading effect on rare earth element
929 binding to humic acid: Experimental and modeling evidence, Geochim. Cosmochim. Acta
930 74, 1749-1761.

931 Marsac R., Davranche M., Gruau G., Bouhnik-Le Coz M. and Dia A. (2011) An improved
932 description of the interactions between rare earth elements and humic acids by modeling:
933 PHREEQC-Model VI coupling. Geochim. Cosmochim. Acta 75, 5625-5637.

934 Marsac R., Davranche M., Gruau G., Dia A. and Bouhnik-Le Coz M. (2012) Aluminium
935 competitive effect on rare earth elements binding to humic acid. Geochim. Cosmochim.
936 Acta 89, 1-9.

937 Marsac R., Davranche M., Gruau G., Dia A., Pédrot M., Bouhnik-Le Coz M. and Briant N.
938 (2013) Effects of Fe competition on REE binding to humic acid: Origin of REE pattern
939 variability in organic waters. Chem. Geol. 342, 119-127.

940 Martell A.E. and Hancock R.D. (1996) Metal Complexes in Aqueous Solutions. New York:
941 Kluwer.

942 Milne C. J., Kinniburgh D. G. and Tipping E. (2001) Generic NICA-Donnan model parameters
943 for proton binding by humic substances. Environ. Sci. Technol. 35, 2049-2059.

944 Milne C. J., Kinniburgh D. G., Van Riemsdijk W. H. and Tipping E. (2003) Generic NICA-
945 Donnan model parameters for metal-ion binding by humic substances. Environ. Sci.
946 Technol. 37, 958–971.

947 Montenegro A. C., Orsetti S. and Molina F. V. (2014) Modelling proton and metal binding to
948 humic substances with the NICA–EPN model. Environ. Chem. 11, 318-332.

949 Moore R. C., Borkowski M., Bronikowski M. G., Chen J.-F., Pokrovsky O. S., Xia Y. and
950 Choppin G. R. (1999) Thermodynamic modeling of actinide complexation with acetate
951 and lactate at high ionic strength. J. Sol. Chem. 28, 521-531.

952 Mühlenweg U., Brasser Th. and Hertes U. (1997) Charakterisierung von mineralisierten
953 Tiefengrundwässern in nichtsalinaren Festgesteinen. Report GRS-144, ISBN 3-931995-
954 04-6, Gesellschaft für Anlagen- und Reaktorsicherheit (GRS) mbH, Germany. p. 19

955 Parkhurst D. L. and Appelo C. A. J. (1999) User's guide to PHREEQC (Version 2) - a computer
956 program for speciation, batch reaction, one-dimensional transport and inverse
957 geochemical calculation. Water-resources Investigation Report 99–4259, USGS, Denver,
958 Colorado, p. 312.

959 Pinheiro J. P., Mota A. M. and Benedetti M. F. (2000) Effect of aluminum competition on lead
960 and cadmium binding to humic acids at variable ionic strength. Environ. Sci. Technol. 34,
961 5137-5143.

962 Pitzer K. S. (1991) Ion interaction approach: theory and data correlation. In: Pitzer, K.S. (Ed.),
963 Activity Coefficients in Electrolyte Solutions. CRC Press, Boca Raton, Florida, pp. 75-
964 153.

965 Rey-Castro C., Lodeiro P., Herrer R. and Sastre De Vicente M. E. (2003) Acid-base properties of
966 brown seaweed biomass considered as a Donnan gel. A model reflecting electrostatic
967 effects and chemical heterogeneity. Environ. Sci. Technol. 37, 5159-5167.

968 Ringböm A. (1963) Complexation in Analytical Chemistry. Interscience, New York.

969 Ritchie J. D. and Perdue E.M. (2003) Proton-binding study of standard and reference fulvic acids,
970 humic acids, and natural organic matter. Geochim. Cosmochim. Acta 67, 85-96.

971 Sasaki T., Kobayashi T., Tagagi I. and Moriyama H. (2008) Discrete fragment model for
972 complex formation of europium(III) with humic acid. J. Nucl. Sci. Technol. 45(8), 718–
973 724.

974 Schijf J. and Ebling A. M. (2010) Investigation of the ionic strength dependence of Ulva lactuca
975 acid functional group pKas by manual alkalimetric titrations. Environ. Sci. Technol. 44,
976 1644–1649.

977 Schnurr A., Marsac R., Kupcik T., Rabung T., Lützenkirchen J. and Geckeis H. (2015) Sorption
978 of Cm(III) and Eu(III) onto clay minerals under saline conditions: Batch adsorption,
979 Laser-fluorescence spectroscopy and modeling. Geochim. Cosmochim. Acta 151, 192-
980 202.

981 Stockdale A., Tipping E., Hamilton-Taylor J. and Lofts S. (2011) Trace metals in the open
982 oceans: speciation modelling based on humic type ligands. Environ. Chem. 8(3), 304-319.

983 Szabò G., Guczi J., Reiller P., Miyajima T. and Bulman R. A. (2010) Effect of ionic strength on
984 complexation of Pu(IV) with humic acid. Radiochim. Acta 98, 13–18.

985 Tipping E. (1998) Humic ion-binding model VI: an improved description of the interactions of
986 protons and metal ions with humic substances. Aquat. Geochem. 4, 3–48.

987 Tipping E. and Hurley M. A. (1992) A unifying model of cation binding by humic substances.
988 Geochim. Cosmochim. Acta 56, 3627–3641.

989 Tipping E., Lofts S. and Sonke J. (2011) Humic ion-binding Model VII: a revised
990 parameterisation of cation-binding by humic substances. Environ. Chem. 8, 225-235.

991 Tipping E., Rey-Castro C., Bryan S. E. and Hamilton-Taylor J. (2002) Al(III) and Fe(III) binding
992 by humic substances in freshwaters and implications for trace metal speciation. Geochim.
993 Cosmochim. Acta 66, 3211–3224

994 Torres R. A. and Choppin G. R. (1984) Europium(III) and Americium(III) stability constants
995 with Humic acid. Radiochim. Acta 35(3), 143-148.

996 Turner A., Pedroso S. S. and Brown M. T. (2008) Influence of salinity and humic substances on
997 the uptake of trace metals by the marine macroalga, Ulva lactuca: Experimental
998 observations and modelling using WHAM. Mar. Chem. 110, 176–184.

999 van Dijk H. Z. (1959) Zur Kenntnis der Basenbindung von Huminsäuren. Pflanzenernähr. Düng.
1000 Bodenk. 84, 150-155.

1001 van Leeuwen H. P. and Town R. M. (2016) Electric condensation of divalent counterions by
1002 humic acid nanoparticles. Environ. Chem. 13, 76-83.

1003 Wall N. A. and Choppin G. R. (2003) Humic acids coagulation: influence of divalent cations.
1004 Appl. Geochem. 18, 1573–1582.

1005 Wall N. A., Borkowski M., Chen J.-F. and Choppin G. R. (2002) Complexation of americium
1006 with humic, fulvic and citric acids at high ionic strength. Radiochim. Acta 90, 563–568.

1007 Zoll A. M. and Schjif J. (2012) A surface complexation model of YREE sorption on Ulva lactuca
1008 in 0.05–5.0 M NaCl solutions. Geochim. Cosmochim. Acta 97, 183–199.

1009

Table and figure captions:

Table 1. Summary of the experimental conditions for the M-HA complexation experiments of Wall et al. (2002) (Am^{3+}), Labonne-Wall et al. (1999) (UO_2^{2+}), Kurk and Choppin (2000) (Co^{2+} and Ni^{2+}) and Laszak and Choppin (2001) (Ca^{2+}).

Figure 1. a) Surface potential (Ψ_0) and Donnan potential (Ψ_D) calculated for Model VII and NICA-Donnan, respectively, for pH (= - log a_{H^+}) = 5.5 versus the ionic strength. The y-axis for Ψ_D is shifted by 60 mV compared with the one of Ψ_0 to highlight their similar evolution with *I*. (b) Activity coefficient of the proton ($\log \gamma_{H^+}$) versus *I* in NaCl, $NaClO_4$ and $NaNO_3$ solutions, calculated with SIT. (c) HA charge versus pH_m in 0.1 M (black curve), 1 M (blue curve), and 3 M (red curve) [0.1, 1.051, 3.503 m, respectively] $NaClO_4$. Points are experimental results of Maes et al. (1992) and lines are results from Model VII. (For interpretation to references to color, the reader is referred to the web version of this article.)

Figure 2. (a) Experimental Am-HA binding isotherms of Czerwinski et al. (1996) for pH_m = 6 and m_{NaClO_4} = 0.01, 0.1, 1 and 3.5 m (symbols) compared with simulations using Model VII (lines). Experimental (b) log $^{HA}\beta_{LC}$ and (c) loading capacity (*LC*) values for Am compared with Model VII and NICA-Donnan predictions versus *I* ($NaClO_4$) in the experimental conditions of Czerwinski et al. (1996). Experimental error bars are generally smaller than the symbols.

Figure 3. Experimental binding capacity (B_{max}) and log $^{HA}\beta(Pu^{4+})$ values of Szabò et al. (2010) versus *I* ($NaClO_4$) compared with Model VII predictions. Arrows refer to the y-axis corresponding to the data. Experimental error bars for B_{max} are generally smaller than the symbols.

Figure 4. (a) Apparent Am-HA and U(VI)-HA complexation constants (Wall et al., 2002; Labonne-Wall et al., 1999) versus *I* (NaCl) for pH_m = 5.1 and 4.9, respectively. (b) Apparent M-HA complexation constants (M = Ni^{2+} or Co^{2+}, Kurk and Choppin, 2000) versus *I* (NaCl) for pH_{exp} = 6. For both figures, lines are predictions by Model VII (full line) and NICA-Donnan (dashed lines) using the generic parameters (but shifted down for the case of Am-HA, see text for details). Experimental error bars are commonly smaller than the symbols.

Figure 5. Experimental apparent Ca^{2+}-HA complexation constants versus pH_m for I = 0.1, 1 and 3 m NaCl (Laszak and Choppin, 2001) compared with (a) Model VII (simulated curves for I = 1 and 3 m NaCl overlap) and (b) NICA-Donnan predictions. Experimental error bars are commonly smaller than the symbols on all three figures.

Figure 6. (a) Experimentally observed effect of the ionic strength on Am-HA complexation at low (Wall et al., 2002; pH_m = 5.1; NaCl) and high metal loading (Czerwinski et al., 1996; pH_m = 6; $NaClO_4$). (b) Simulated effect of the ionic strength on Am-HA complexation at low ($[Am]_{tot}$ = 10^{-9} m) and high metal loading ($[Am]_{tot}$ = 10^{-6} m) with Model VII (black curves) and NICA-Donnan (blue curves) in NaCl for a HA concentration of 1 mg L^{-1} and pH = 5.5. (For interpretation to references to color, the reader is referred to the web version of this article.)

	[M] (mol L^{-1})	[HA] (mg L^{-1})	m_{NaCl} (m)	pH	pH buffer
Am^{3+}	1×10^{-9}	1 - 10	0.1 - 6	5.1 (pH_m)	10^{-2} M acetate
UO_2^{2+}	5.24×10^{-7}	2 - 10	0.1 - 6	4.9 (pH_m)	10^{-2} M acetate
Ni^{2+}	1×10^{-9}	2×10^{-3} - 1.6×10^{-2}	0.3 - 5	6.0 (pH_{exp})	No
Co^{2+}	1×10^{-10}	1.3×10^{-2} - 2.2×10^{-1}	0.3 - 5	6.0 (pH_{exp})	No
Ca^{2+}	1×10^{-8}	0 - 500	0.1 - 3	4.5 - 9.5 (pH_m)	No

Table 1

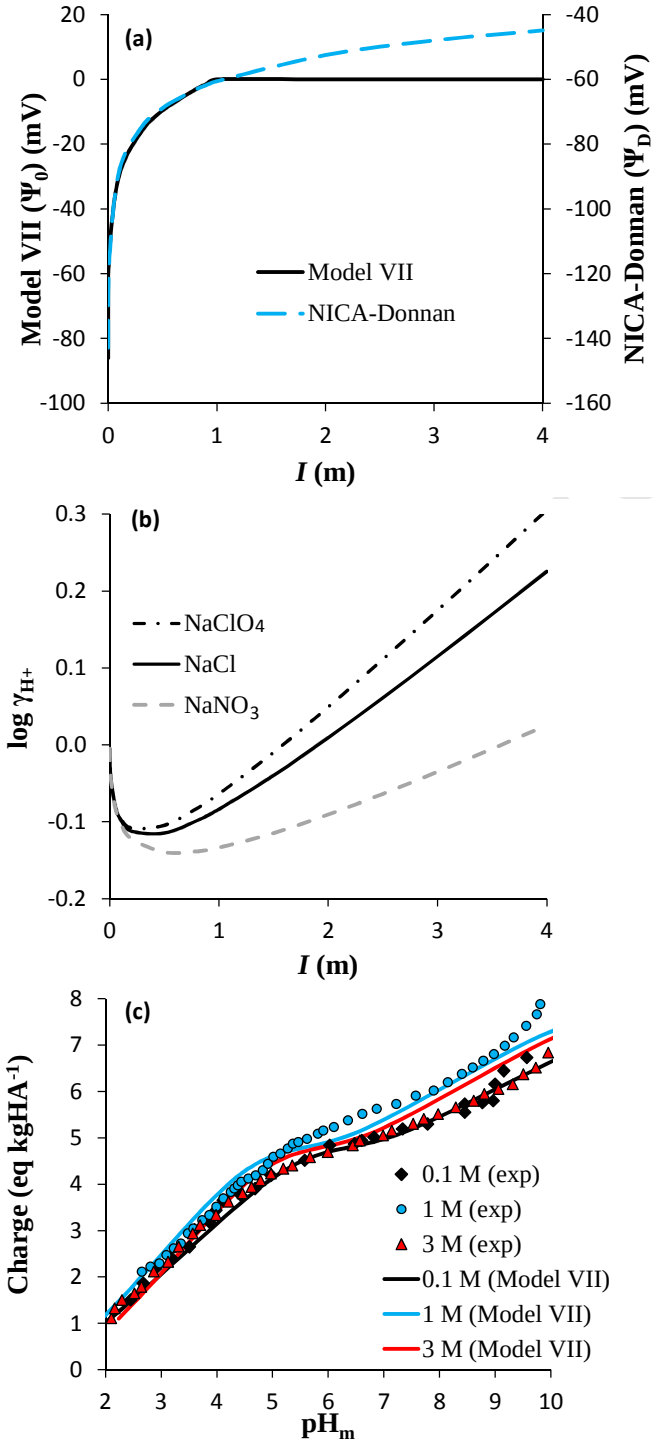

1053

1054

1055 **Figure 1**

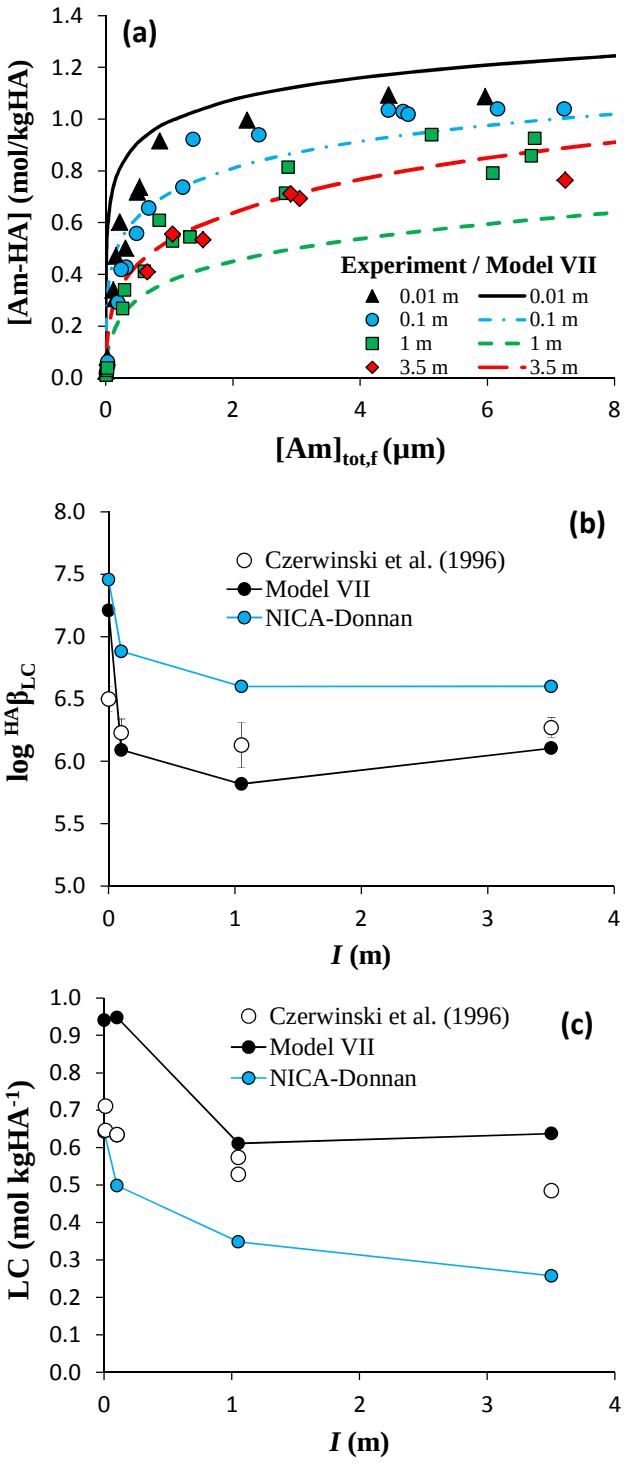
(a)
[Am-HA] (mol/kgHA)
[Am]tot,f (µm)
Experiment / Model VII
0.01 m
0.1 m
1 m
3.5 m
0.01 m
0.1 m
1 m
3.5 m
(b)
Czerwinski et al. (1996)
Model VII
NICA-Donnan
log HAβLC
I (m)
(c)
Czerwinski et al. (1996)
Model VII
NICA-Donnan
LC (mol kgHA-1)
I (m)

Figure 2

1062

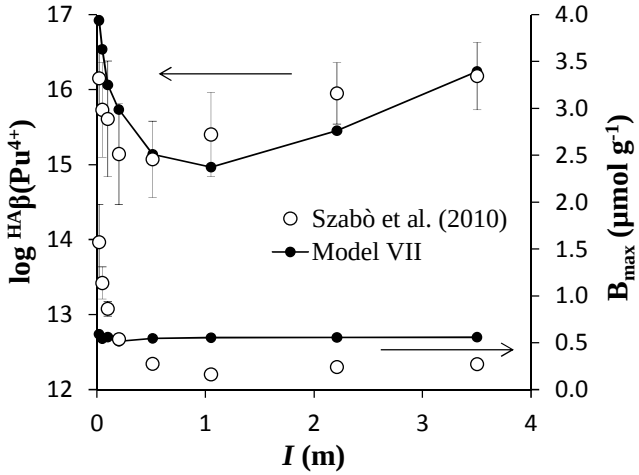

1063

1064 **Figure 3**

1065

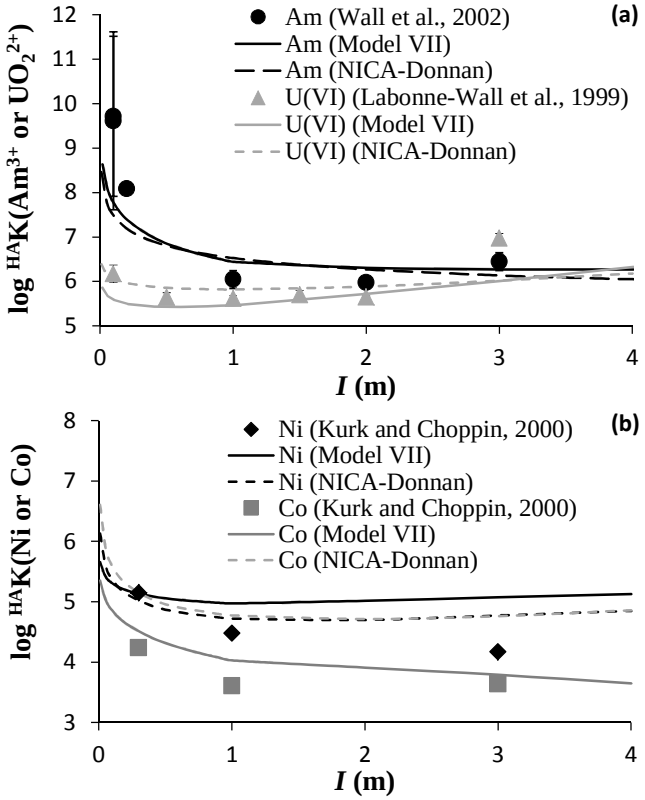

1066

1067

1068 **Figure 4**

1069

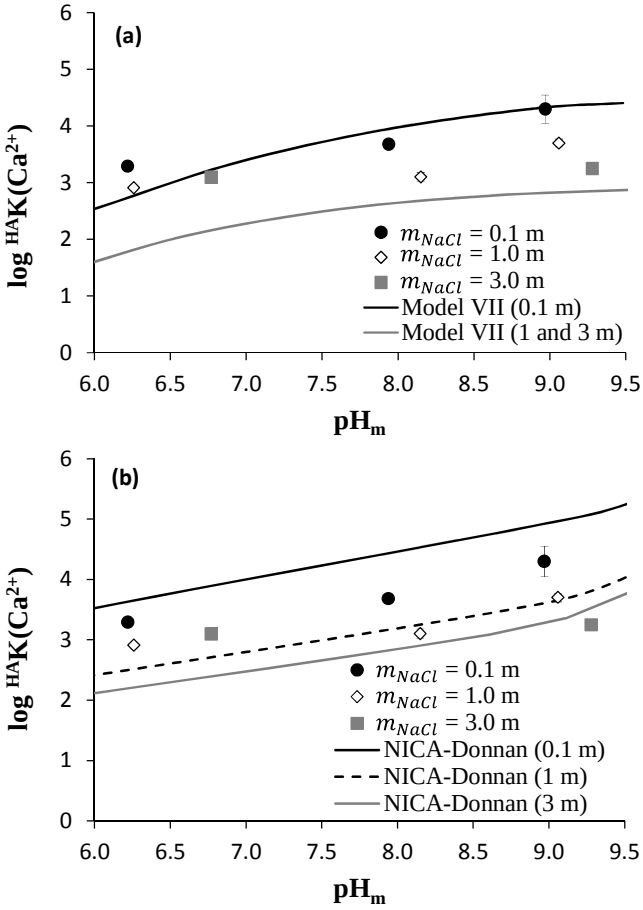

1070

1071

1072 **Figure 5**

1073

1074

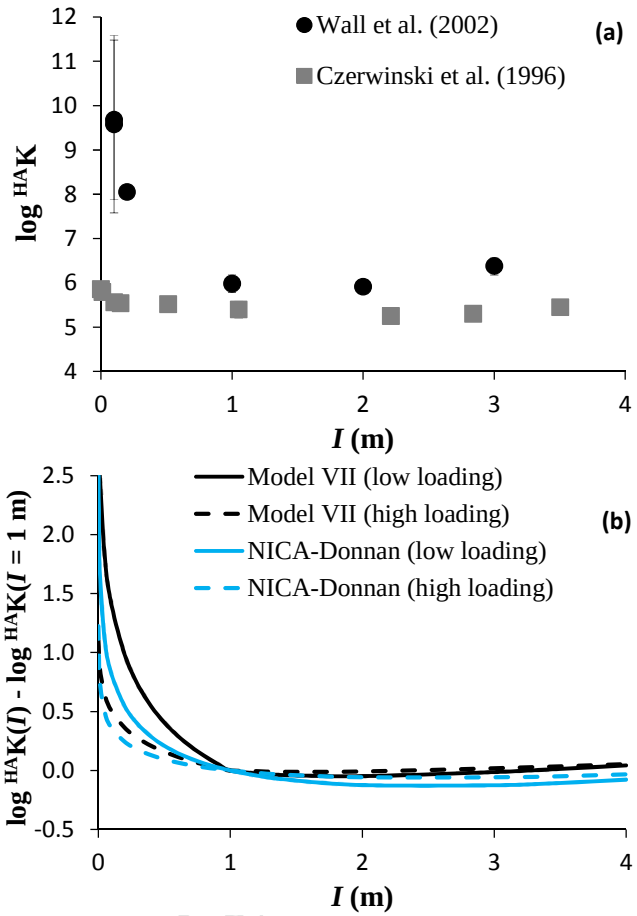

1075

1076 **Figure 6**